Phil. Trans. R. Soc. Lond. B **296**, 47–54 (1981)
Printed in Great Britain

Topology of morphologically detectable protein and cholesterol in membranes of polypeptide-secreting cells

By L. Orci, M. Amherdt, R. Montesano, P. Vassalli† and A. Perrelet

Institute of Histology and Embryology and †Department of Pathology, University of Geneva, 1211 *Geneva* 4, *Switzerland*

[Plates 1–10]

The freeze–fracture morphology of intracellular and plasma membranes in endocrine and exocrine polypeptide-secreting cells has been studied to detect changes while these membranes interact during secretion. A qualitative and quantitative evaluation of intramembrane particles and filipin binding as indicators of protein and cholesterol content of the membranes, respectively, reveals the following changes. From the forming of the maturing pole of the Golgi complex, membranes lose morphologically detectable protein and gain morphologically detectable cholesterol. The protein-poor, cholesterol-rich secretory granule membrane then interacts with a richly particulate plasma membrane in endocrine cells and with a moderately particulate luminal membrane in exocrine cells. The site of interaction between secretory granule and plasma membrane is characterized by a local clearing of intramembrane particles; by contrast, filipin-binding sites revealing cholesterol are present in this area. In exocrine cells, the fused secretory granule, which is initially rich in filipin–cholesterol complexes and poor in particles, appears to lose progressively its filipin labelling to resemble the poorly labelled luminal membrane. These findings, although they cannot be interpreted definitely at present, clearly show impressive changes of membrane structure along the secretory pathway and suggest that a corresponding degree of functional specialization is needed for proper interaction to occur.

When preparing the written account of this contribution we were faced with the alternative of elaborating a fully edited text or maintaining some of the structure and wording used in the oral presentation. We chose the latter alternative with the merits and pitfalls of such a direct and sketchy, although more vivid, approach.

The plasma membrane, once believed to be a rather rigid envelope of cells, has become, in the eyes of cell biologists, a differentiated fluid mosaic (Singer & Nicolson 1972) in dynamic equilibrium with other membrane segments situated inside the cell. This view has emerged mainly from the study of polypeptide-secreting cells where the secretory product is enclosed within an intracellular membrane compartment which itself becomes part of the plasma membrane during polypeptide release (for review see Palade 1975). The various membrane compartments, although functionally continuous, differ widely in their chemical composition and morphological appearance (for review see Meldolesi *et al.* 1978); nevertheless, the membranes that interact directly are believed to share some common properties. It is the purpose of this paper to present a morphological approach towards this issue with the aid of endocrine and exocrine polypeptide-secreting cells as examples.

Endocrine pancreas (β-cell)

(*a*) *Golgi apparatus*

As far as membrane interactions are concerned, three main stations can be recognized along the secretory pathway of the insulin-secreting cell or β-cell (Orci 1974) (figure 1*a*, *b*): (1) the budding and subsequent addition of rough endoplasmic reticulum (RER)-derived microvesicles to the forming pole of the Golgi apparatus, (2) the release of membrane-bound vesicles (or secretory granules) containing packed secretory product from the maturing Golgi pole, and (3) the addition of secretory granule membrane to the plasma membrane during exocytosis (for reviews see Palade (1975) and Borgese *et al.* (1979)).

The ordered transit of different polypeptides across the Golgi cisternae, their sorting out and their packaging at correct addresses within individual membrane sacs require a high degree of specialization. A great deal of effort has been spent in detecting specialized areas within the Golgi apparatus at both biochemical and ultrastructural levels (for recent reviews see Whaley & Dauwalder (1979) and Tartakoff (1980)); so far, however, heterogeneity in the membranes of different cisternae has not been completely documented. A most useful approach to the morphological analysis of membranes has become, over the last decade, the technique of freeze–fracture (for review see McNutt 1977). Whereas in highly magnified thin sections for electron microscopy, cell membranes appear invariably as two dense lines separated by a clear space, with some variations in their respective width and electron density (Robertson 1959), freeze–fractured membranes show a more differentiated morphology, composed of a smooth background interrupted by globular subunits, the intramembrane particles (Branton 1969; Deamer 1977) (figures 2 and 3). It has been demonstrated that the smooth zones correspond to the lipidic domain of the membrane, while the particles represent, at least in part, membrane integral proteins (Yu & Branton 1976).

Recently it has been possible to localize one of the essential components of the lipid domain, cholesterol. This localization relies on the use of a polyene antibiotic, filipin, which specifically interacts with cholesterol and related 3-β-hydroxysterols resulting in the formation of multimolecular filipin–cholesterol complexes (Norman *et al.* 1972; De Kruijff *et al.* 1974; Norman *et al.* 1976). These complexes are readily detectable as *ca.* 25 nm protuberances (or smaller pits) in freeze–fracture replicas (Verkleij *et al.* 1973; Tillack & Kinsky 1973; Elias *et al.* 1979; Montesano *et al.* 1979; Robinson & Karnovsky 1980) and they are thus easily distinguishable by their size from the much smaller protein particles (averaging 8 nm in diameter). On this background, we shall first consider the protein component of Golgi membranes.

Description of plate 1

Figure 1. (*a*) Pancreatic β-cell. Thin section showing the main membrane compartments involved in polypeptide secretion: the limiting membrane (see figure 2) of stored secretory granules (SG) originate in the maturing Golgi cisternae (MG); on the opposite side, transitional elements (TE) of the rough endoplasmic reticulum (RER) contribute to the forming Golgi cisternae (FG) through microvesicles (MV). Beside stored secretory granules (SG) there are less-dense granules, the maturing secretory granules (MSG) which are characterized by a coat on part of their limiting membrane (arrows). Other coated membrane segments appear also on Golgi cisternae (arrowhead) and as coated vesicles (CV), present at both the forming and the maturing pole of the Golgi complex. (Magn. × 60000.)

(*b*) Schematic drawing of the three main levels at which membrane interactions occur during polypeptide secretion: 1, contribution of RER-derived microvesicles to formation of Golgi cisternae; 2, detachment of membrane vesicles containing packed secretory product from the maturing Golgi cisternae; 3, fusion of the secretory granule membrane to the plasma membrane allowing the release of the secretory product at the extracellular space. Coated membrane elements are figured on Golgi cisternae, on secretory granules and on individual coated vesicles.

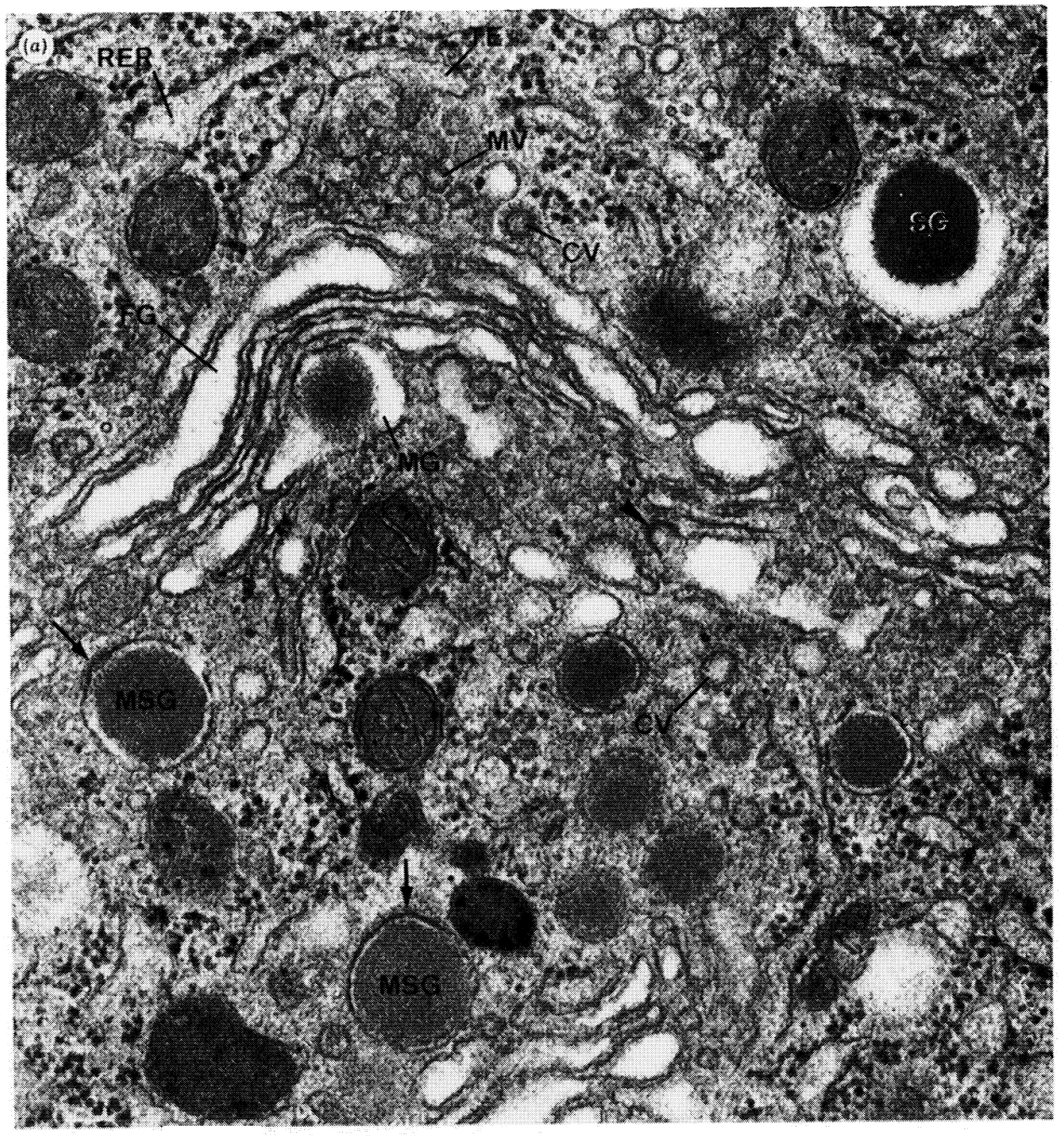

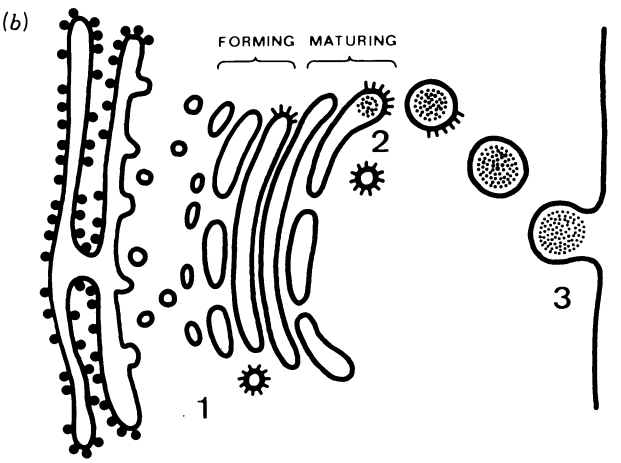

FIGURE 1. For description see opposite.

(*Facing p.* 48)

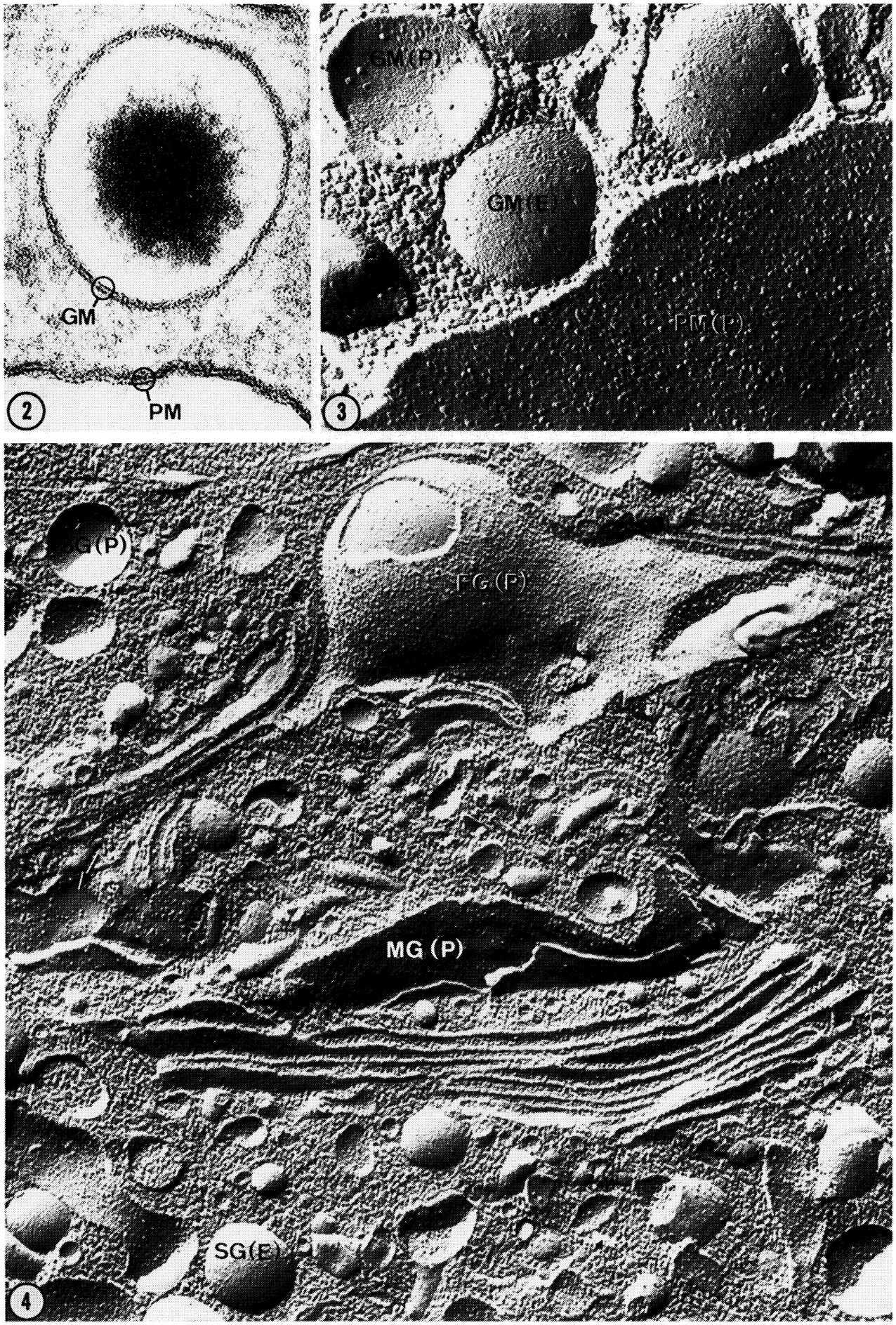

FIGURES 2–4. For description see opposite.

Description of plate 2

Figure 2. Pancreatic β-cell. Thin-section appearance of secretory granule limiting membrane (GM) and plasma membrane (PM). Note the similar aspect of these two membranes and compare with their freeze–fracture morphology (see figure 3). (Magn. × 166000.)

Figure 3. Pancreatic β-cell. Freeze–fracture appearance of the cytoplasmic (protoplasmic) leaflet of the plasma membrane (PM(P)) and of the granule limiting membrane: outer or protoplasmic leaflet (GM(P)); inner or exoplasmic leaflet (GM(E)). Quantitation of intramembrane particles on the plasma membrane shows approximately 2000 particles per square micrometre in the P-leaflet and 300 in the E-leaflet, while the P- and E-leaflets of the granule membrane have 250 and 50 particles per square micrometre, respectively. (Magn. × 105000.)

Figure 4. Pancreatic β-cell. Freeze–fracture replica of the Golgi apparatus showing the decrease in the number of intramembrane particles from the forming (FG(P)) to the maturing (MG(P)) cisternae (protoplasmic leaflets). Note the very low particle content of both secretory granule membrane leaflets (SG(P) and SG(E)). In the maturing cisternae to the left, the arrow indicates the area very poor in particles from which the secretory granule membrane will eventually arise. (Magn. × 64000.) (Courtesy of *Diabetologia* (Orci 1974).)

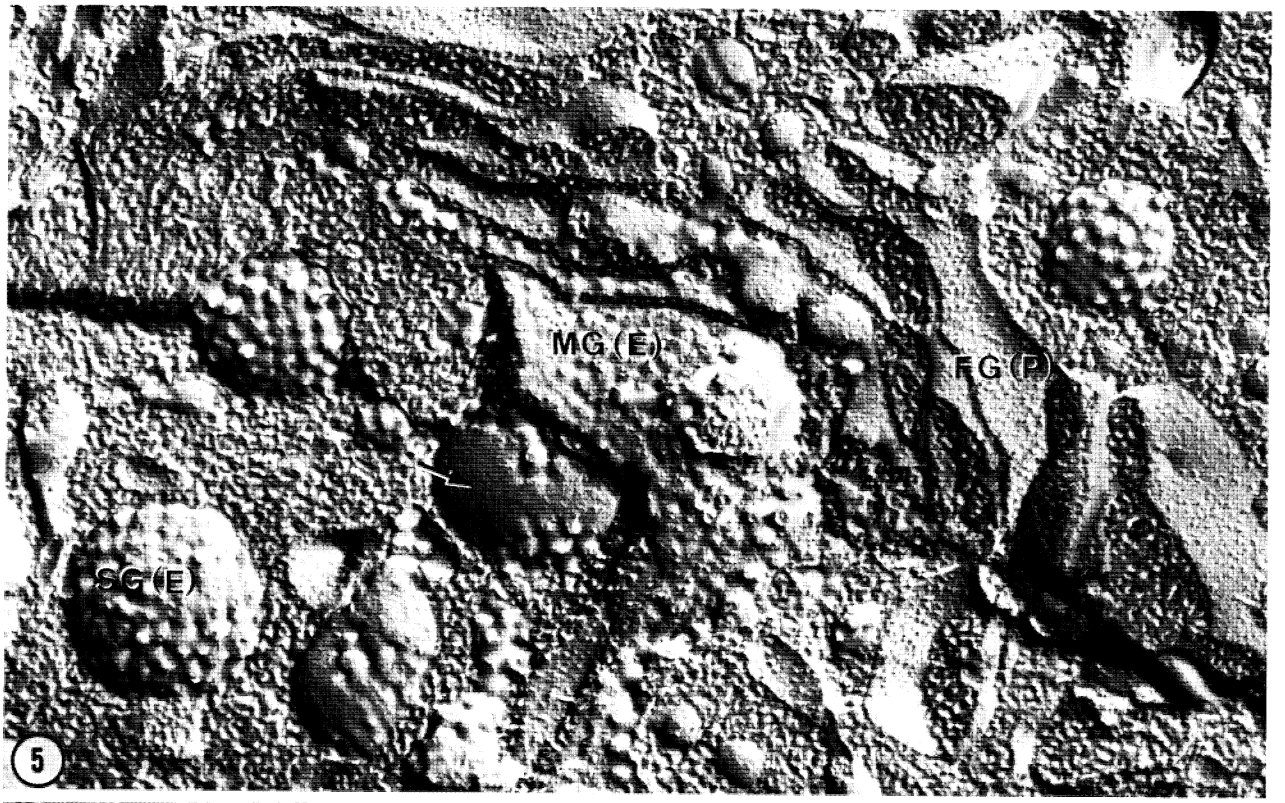

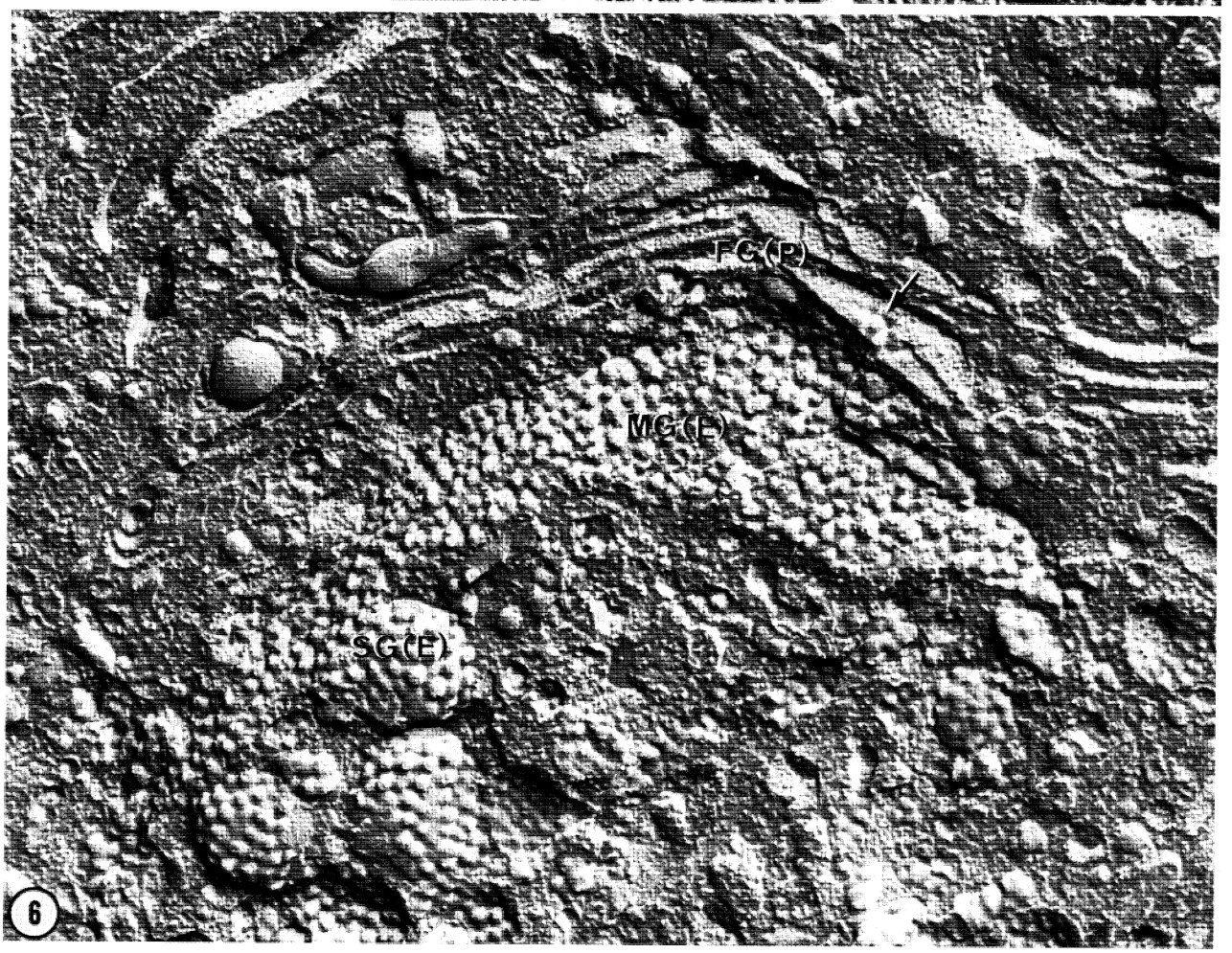

FIGURES 5 AND 6. For description see opposite.

In a freeze–fracture replica of the Golgi apparatus of a pancreatic β-cell without filipin treatment (figure 4), a marked difference can be observed in the density of intramembrane particles across the Golgi cisternae. The quantitative evaluation of these particles shows that the forming cisternae contain approximately 3000 particles per square micrometre of P-face, the maturing cisternae about 800, and the secretory granules about 250. However, variations in the density of intramembrane particles occur not only from one cisterna to another, but also within the same cisterna. An example is shown in figure 4, where a maturing cisterna displays an abrupt drop in the number of protein particles. This particle-poor area will eventually envelop the packed secretory product (cf. figure 1). Thus, the movement of membranes from the forming to the maturing pole of the Golgi apparatus is accompanied by a marked reduction of the particle (protein) content of these membranes. If we now examine the Golgi apparatus in cells treated with filipin in order to localize cholesterol, the reverse pattern can be observed. It should be first pointed out that the pre-Golgi compartment, the transitional elements of the rough endoplasmic reticulum, is virtually devoid of filipin–cholesterol complexes, while the post-Golgi compartment, the secretory granule membranes, is heavily labelled by filipin. In the Golgi apparatus itself, filipin–cholesterol complexes are numerous in the particle-poor, maturing Golgi cisternae, while the forming cisternae, shown above to be particle–rich, contain very few complexes (figures 5 and 6). The evaluation of the number of filipin–cholesterol complexes per square micrometre of membrane (average of both leaflets) shows 36 complexes in the forming cisternae, 156 in the maturing cisternae and 350 in secretory granule membrane, that is about a tenfold apparent enrichment in morphologically detectable cholesterol (Orci *et al.* 1981). On the basis of such morphological evidence, it can be concluded that the membranes at the two opposite Golgi poles differ not only in their protein but also in their cholesterol content, and that in addition, differences exist from one area to the next within individual cisternae. The existence of such microdomains of cisternal membrane could not be clearly demonstrated on the basis of available methods for Golgi subfractionation and chemical analysis.

An obvious question raised by these data is how the decrease in particles and the increase in cholesterol takes place. There is morphological evidence, at the level of the Golgi apparatus, for specific segments of the cisternal membranes that appear 'coated' in thin sections (figure 1), and particle-rich, cholesterol–poor in freeze–fracture replicas (figures 7–12) (Orci *et al.* 1981). Although at present there is no direct proof that these coated segments detach from cisternae to form coated vesicles, the selective removal of such protein-rich, cholesterol–poor areas from the cisternal membrane could contribute to the change in membrane composition from the forming to the maturing pole of the Golgi apparatus. Newly formed secretory granules (or maturing granules) also have coated segments (see figures 1 and 7) on their limiting membrane, and the selective removal of these segments could result in the further modification of the protein and cholesterol content noticed between the maturing cisternae and the stored secretory granules.

Description of plate 3

Figures 5 and 6. Pancreatic β-cells. Freeze–fracture replicas of the Golgi apparatus after filipin treatment to reveal cholesterol. Filipin–cholesterol (f-c) complexes appear as *ca.* 25 nm protuberances on the membrane fracture face and their distribution across the Golgi complex is markedly asymmetric. Membrane leaflets at the forming pole of the Golgi (FG(P)) show no or very few complexes (arrow, figure 6), while membrane leaflets at the maturing pole (MG(E)), including secretory granule membrane (SG(E)), contain numerous complexes. A maturing cisterna in figure 5 shows an area devoid of filipin labelling (arrow) which probably represents a coated region (see figures 7–12). (Magns: figure 5, × 82000; figure 6, × 65000.) (Figure 5 by courtesy of *Proc. natn. Acad. Sci. U.S.A.* (Orci *et al.* 1981).)

(*b*) *Exocytosis*

The next step in membrane interaction during secretion is that occurring when a secretory granule opens at the cell surface during exocytosis (for a recent review see Orci & Perrelet 1978). For exocytosis to take place, the secretory granule and plasma membranes must come into very close contact to form a so-called pentalaminar structure in which the protoplasmic leaflet of the granule membrane merges with the protoplasmic leaflet of the plasma membrane (Palade & Bruns 1968; Lagunoff 1973; Palade 1975; Lawson *et al.* 1977). The fusion of the residual leaflets then results in the classical image of exocytosis, namely a more or less profound depression of the cell surface surrounding a granule content exposed to the extracellular space (figures 13 and 14). Such images also indicate that two formerly separated membranes become continuous with one another without detectable changes in their thin-section appearance. Thus, one has to turn again to freeze–fracture to gain some information on the structure of the two interacting membranes.

As shown above, the protoplasmic leaflet of the granule membrane has a low particle content, about 250 per square micrometre; by contrast, the protoplasmic leaflet of plasma membrane has a much higher particle content, about 2000 per square micrometre. How do these membranes interact during exocytosis? Figures 15–18 illustrate the proposed sequence of morphological steps underlying exocytosis as seen by freeze–fracture. First, the granule and plasma membranes approach closely, the plasma membrane showing at the contact point a limited area devoid of intramembrane particles (figure 15). The fusion of the respective membrane leaflets then occurs in the particle-deprived area (figure 16), and after the fusion of secretory granule and plasma membranes, circular depressions, still free of particles, appear in the latter membrane (figures 17 and 18). These depressions may contain the presumptive granule core in the process of being extruded (see figure 17) (Orci *et al.* 1977).

Thus, from this morphological evidence and from similar observations made in other systems (for review see Orci & Perrelet 1978), it can be concluded that exocytosis is accompanied by a clearing of intramembrane particles (proteins) at the site of secretory granule and plasma membrane fusion.†

† The occurrence of particle clearing at sites of exocytosis has been considered to be an artefact (Chandler & Heuser 1979, 1980; for review see Plattner 1981) since it was not found in unfixed, unglycerinated cells freeze–fractured by the rapid freezing method. However, until the same cell type, under the same experimental conditions, has been freeze–fractured according to the two techniques and the results carefully and critically compared, we feel that the controversy cannot be considered resolved.

Description of plate 4

Figures 7–12. Endocrine (figures 7 and 8) and exocrine (acinar) (figures 9–12) pancreatic cells. Filipin-treated endocrine and exocrine pancreatic cells show a correspondence between coated segments and cholesterol-poor areas of the secretory granule membrane during maturation. Figure 7 is a thin section of a β-cell showing a maturing secretory granule (MSG) with its characteristic coated membrane segment (underlined). Figure 8 is a freeze–fracture replica of a β-cell after filipin treatment. The membrane of a maturing secretory granule (MSG) appears deprived of f–c complexes in an area (delimited by the dotted line) that is rich in intramembrane particles. This area is believed to correspond to the coated region of the granule membrane (see figure 7). Figures 9–12 are freeze–fracture replicas showing various stages of maturing zymogen granules (MZ) with the characteristic appearance of coated membrane regions. In cells not treated with filipin, coated regions appear as particle-rich depressions on the P-leaflet (arrow, figure 9) or bulges on the E-leaflet (arrows, figure 10). In filipin-treated cells, coated segments appear devoid of f–c complexes on both membrane leaflets (arrows, figures 11 and 12). (Magns: figure 7, × 80000; figure 8, × 69000; figure 9, × 81000; figure 10, × 64000; figure 11, × 84000; figure 12, × 65000.)

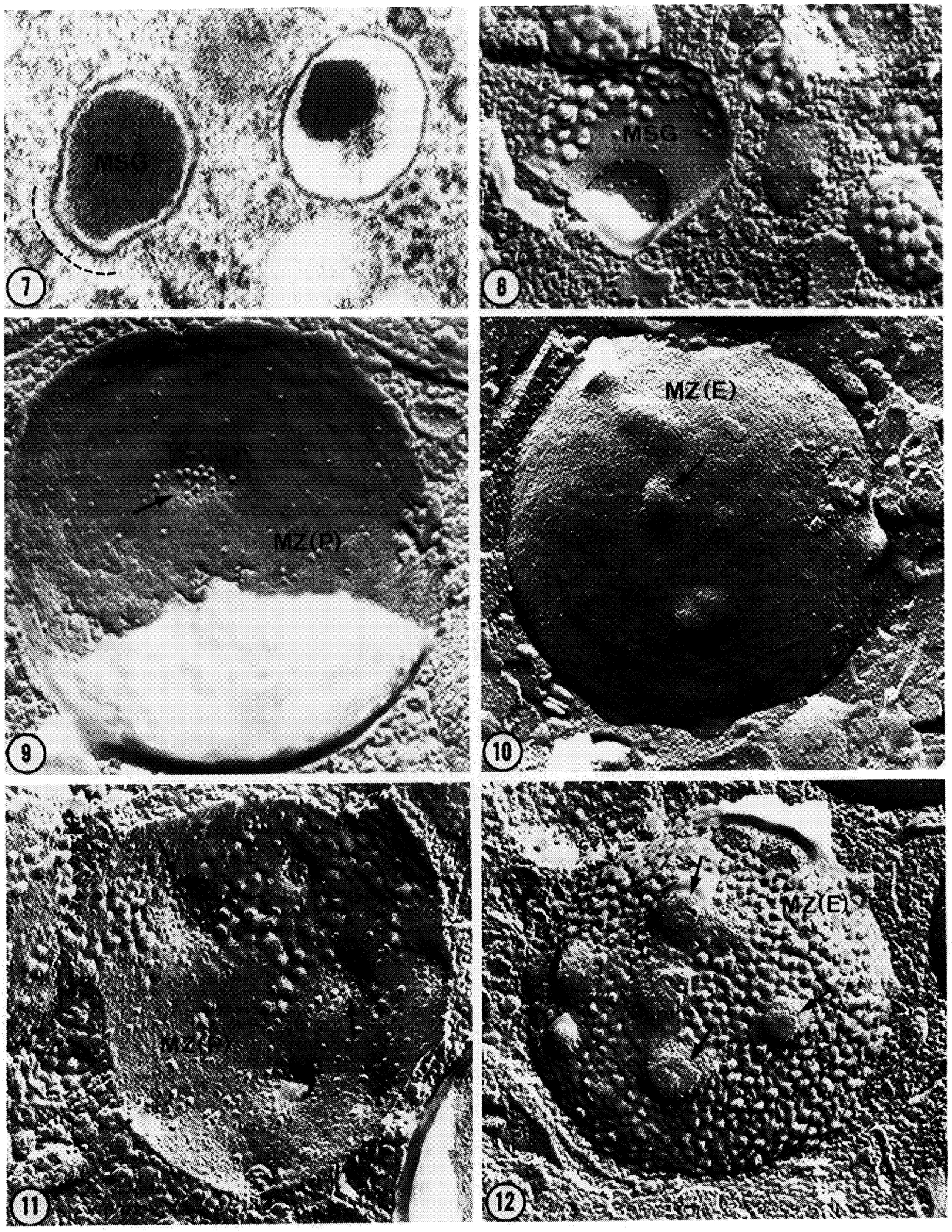

FIGURES 7–12. For description see opposite.

(*Facing p.* 50)

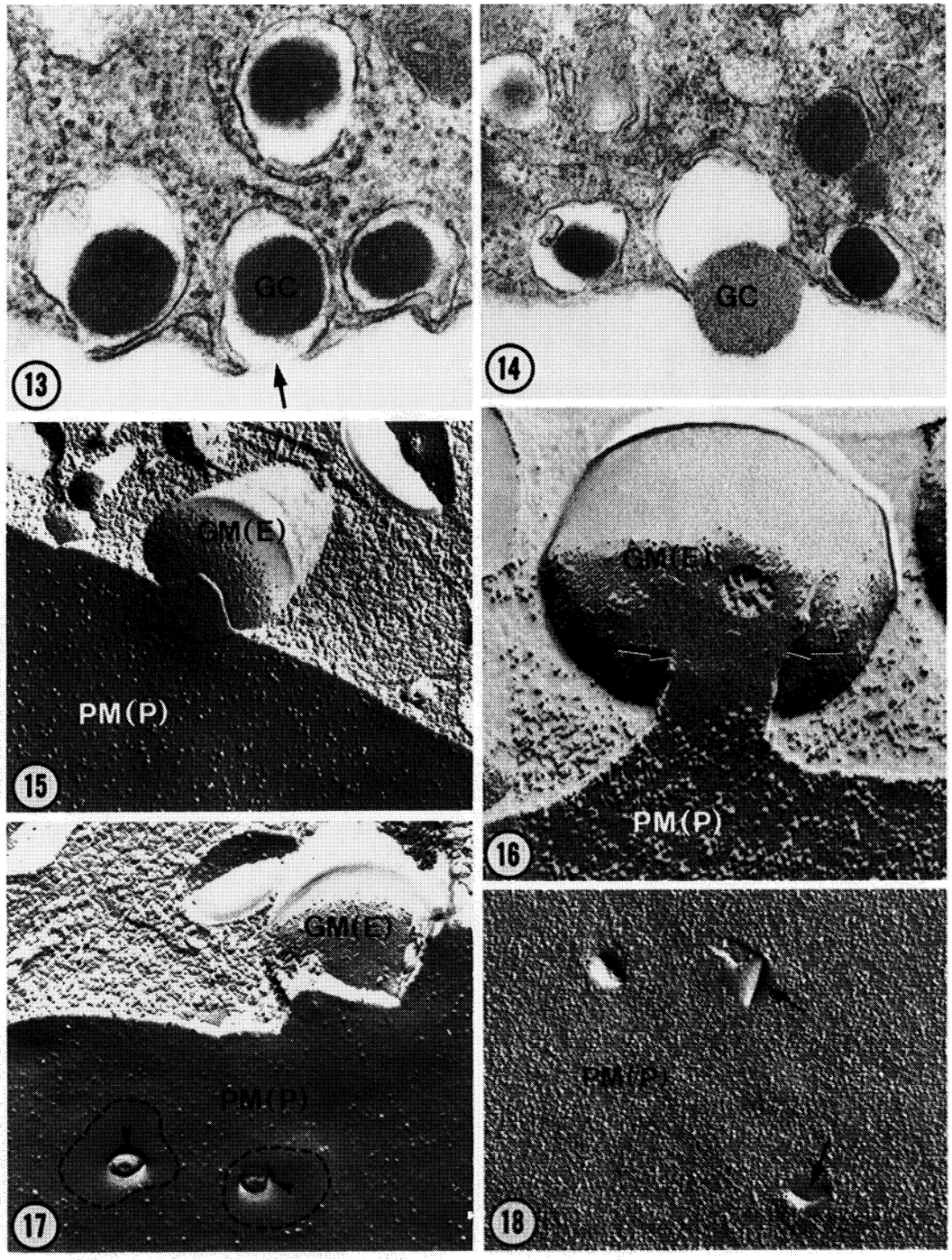

FIGURES 13–18. Pancreatic β-cells. Thin sections (figures 13 and 14) and freeze–fracture images of exocytosis. In thin section, exocytosis appears as a plasma membrane pocket resulting from the merging of the secretory granule membrane with the plasma membrane, exposing the granule core (GC) to the extracellular space. In freeze–fracture specimens of aldehyde-fixed, glycerol-impregnated cells, the pre-fusion stage (figure 15) appears as a particle-free patch (dotted line) in the cytoplasmic leaflet of the plasma membrane (PM(P)) overlying the poorly particulated secretory granule membrane (GM(E)). Figure 16 shows the merging (at the arrows) of the two membranes (GM(E), PM(P)) in a particle-free area; figures 17 and 18 show post-fusion stages in the cytoplasmic leaflet of the plasma membrane (PM(P)). These consist of particle-free patches of various shapes (dotted lines in figure 17; arrow in figure 18). In figure 17, the bulging mass in the particle-free area probably represents extruded granule core material (arrowhead). (Magns: figure 13, × 49000; figure 14, × 43000; figure 15, × 71000; figure 16, × 81000; figure 17, × 67000; figure 18, × 44000.) (Figures 13–15, 17 and 18 by courtesy of *J. Cell Biol.* (Orci *et al.* 1977); figure 16 by courtesy of Elsevier/North-Holland (Orci & Perrelet 1978).)

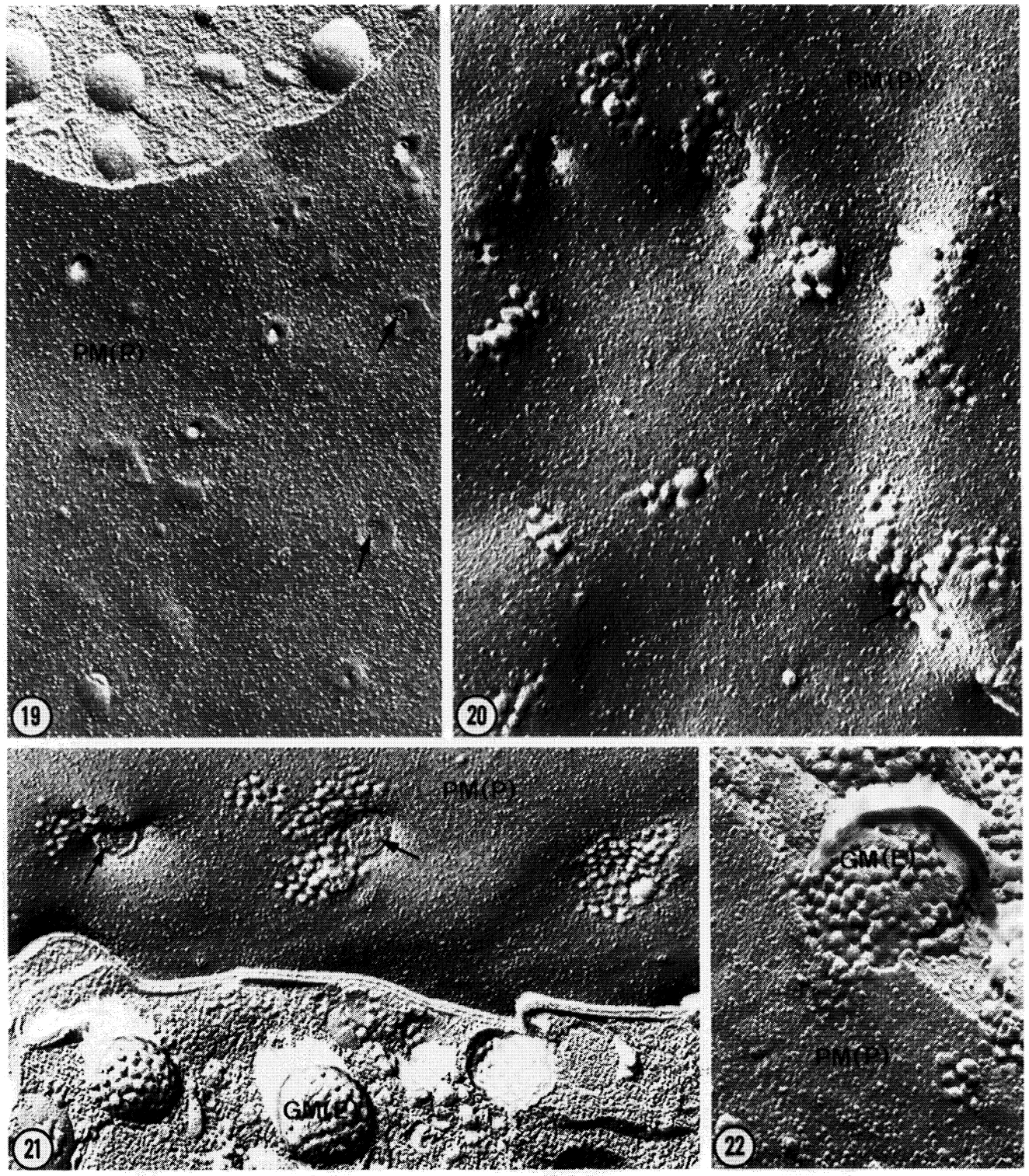

FIGURES 19–22. Pancreatic β-cells. Figure 19 is a freeze–fracture replica showing numerous exocytotic sites (arrows) in the plasma membrane (PM(P)) of a cell not treated with filipin. Figures 20 to 22 show similar images in filipin-treated cells. In these sparsely labelled membranes (PM(P)), f–c complexes occur around exocytotic openings (arrows). Note the richly labelled secretory granule (GM(E)) membrane in figure 21. Figure 22 shows the merging of a filipin-labelled granule membrane (GM(E)) with the plasma membrane (PM(P)) in a filipin-containing region (see figure 15 for a similar image in untreated β-cells). (Magns: figure 19, × 52000; figure 20, × 77000; figure 21, × 47000; figure 22, × 70000.)

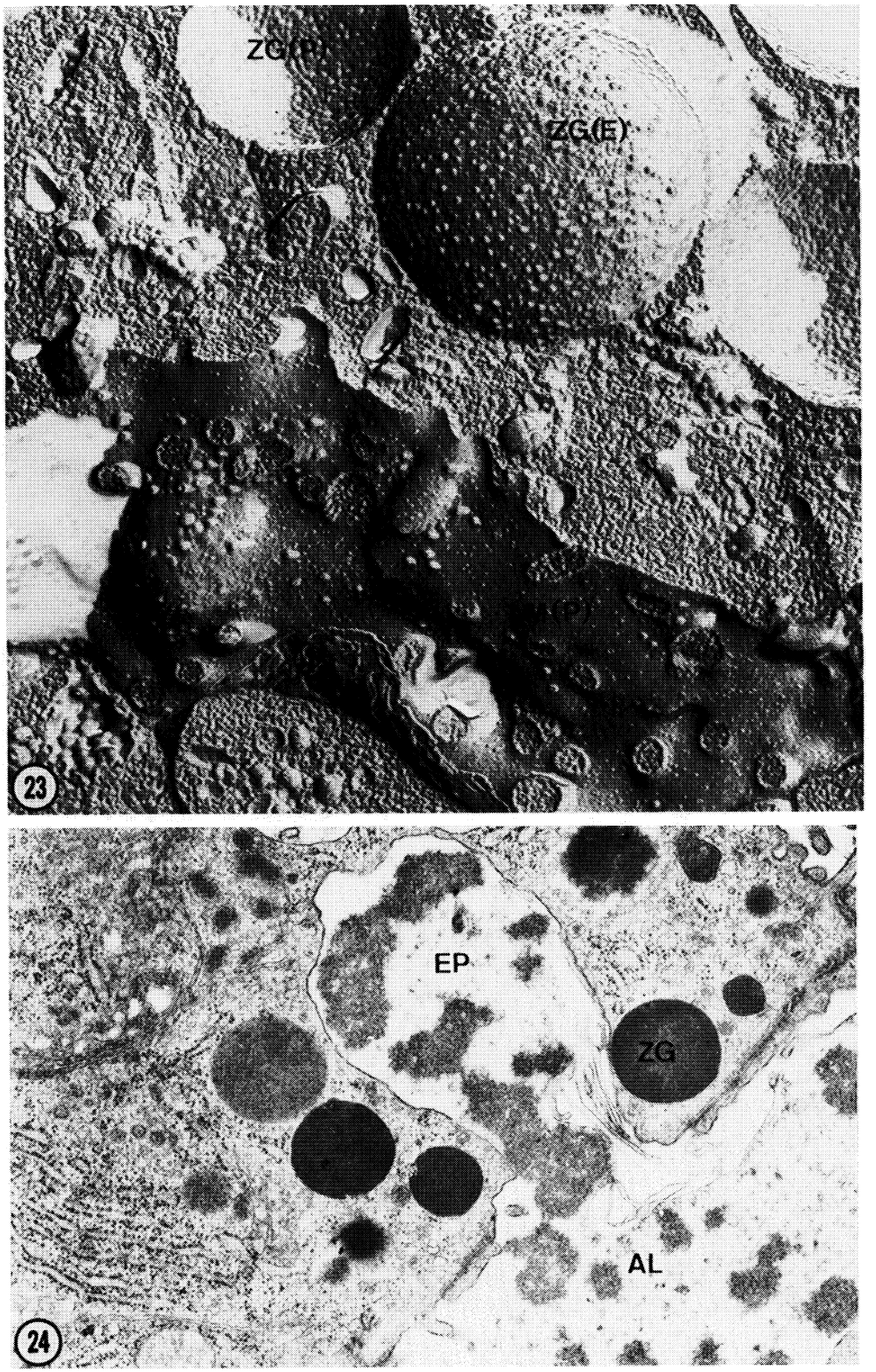

FIGURES 23 AND 24. For description see opposite.

What about cholesterol? The study of membrane changes at exocytotic sites with the cytochemical probe for cholesterol, filipin, has proved more ambiguous to interpret than the data concerning intramembrane particles: after incubation of β-cells (within isolated islets of Langerhans) with filipin, plasma membranes were not homogeneously labelled: heavily labelled membranes juxtaposed to virtually unlabelled membranes of adjacent endocrine cells were frequently observed; in addition, heterogeneity of labelling was observed within individual membranes, consisting most frequently in a patchy distribution of filipin–sterol complexes in the fracture face of the membrane. These various patterns of labelling are not clearly understood at present and therefore render difficult the interpretation of membrane labelling at specific sites. Nevertheless, exocytotic sites appeared consistently in filipin-labelled areas (figures 19–22). This suggests that exocytotic sites contain cholesterol, an interpretation strengthened by observations in other tissues (pancreatic and parotid acinar cells, see below) (Montesano *et al.* 1980; Orci *et al.* 1980), with the exception of the guinea-pig sperm in which filipin–cholesterol complexes seem to be lost from sites of membrane fusion during the acrosomal reaction (Friend 1980).

Exocrine pancreas and parotid gland

(*a*) *Golgi apparatus*

As far as the freeze–fracture morphology of intracellular membranes along the secretory pathway is concerned, a pattern comparable with that described above for the pancreatic β-cell is detectable in pancreatic acinar cells. Forming Golgi membranes contain approximately 1560 particles per square micrometre of P-face and 4 filipin–cholesterol (f–c) complexes (average of both leaflets); the maturing Golgi membranes, including condensing vacuoles, have approximately 620 particles and 168 f–c complexes; the zymogen granule membranes, approximately 110 particles and 196 f–c complexes per square micrometre of P-face. As previously reported (De Camilli *et al.* 1974), particles are less numerous on the luminal than on the lateral membrane of the acinar cell (approximately 380 and 1500 particles per square micrometre of P-face, respectively).

(*b*) *Exocytosis*

In pancreatic and parotid acinar cells, exocytosis is restricted to the apical or luminal domain of the plasma membrane. Figure 23 shows the apical pole of a freeze–fractured pancreatic acinar cell treated with filipin. As in the β-cell, the secretory granule membrane appears labelled with

Description of plate 7

Figure 23. Pancreatic acinar cell. Freeze–fracture replica of the apical pole of a cell treated with filipin. Filipin treatment was carried out by incubating aldehyde perfusion-fixed tissue in the same fixative solution containing 300 μM filipin (a gift of Dr J. E. Grady, Upjohn Company, Kalamazoo) dissolved in 1% (final concentration) dimethylsulphoxide. For incubation, the fixed tissue was chopped into 20 μm slices with an Oxford Vibratome (Oxford Laboratories, San Mateo, California) to facilitate filipin penetration. Both leaflets of the zymogen granule membrane (ZG(E) and ZG(P)) are heavily labelled with filipin-sterol complexes, while the protoplasmic leaflet of luminal plasma membrane (LM(P)) shows only a sparse labelling; circular interruptions in the luminal membrane face represent cross-fractures of microvilli. (Magn. × 42000.)

Figure 24. Pancreatic acinar cell stimulated for 5 min with an intraperitoneal injection of pilocarpine (60 mg/kg) before aldehyde perfusion fixation through the duct system. Thin section of the apical pole showing a large invagination of the luminal plasma membrane opened in the acinar lumen (AL). Electron-dense material represents released secretory product. The large size of the invagination, called an exocytotic pocket (EP), suggests that it results from the addition of several zymogen granules (ZG) to one another and to the luminal membrane. (Magn. × 21000.)

numerous filipin–sterol complexes. However, the apical plasma membrane is only sparsely labelled or not labelled.† As shown in figure 24, stimulation of secretion with pilocarpine induces exocytosis, which results in the formation of large invaginations of the apical pole derived from the incorporation of several zymogen granule membranes into the luminal membrane. These invaginations, or exocytotic pockets, are continuous with the acinar lumen and show in thin sections a material of lower electron density than that present in unopened zymogen granules. In freeze–fracture replicas of stimulated acinar cells treated with filipin (figures 25 and 26), exocytotic pockets opened at the sparsely labelled or unlabelled luminal membrane show various degrees of filipin labelling: labelling may be dense and homogeneous up to the neck of the pocket where it merges with the luminal membrane (figure 25), it can be restricted to the distal half of the pocket, far from its opening (figure 26), or in some cases it may be completely absent except for a few patches of filipin–cholesterol complexes (not shown). Similar images were also found in parotid acinar cells stimulated with isoprenalin and treated with filipin (figures 27–30). In the latter cells, regions of the exocytotic pocket membrane appeared in thin sections to be extensively coated on their cytoplasmic surface (figure 27), while the freeze–fractured luminal membrane showed a patchwork of filipin–cholesterol complex aggregates and intramembrane particle clusters (figure 28).‡

These data suggest that richly labelled exocytotic pockets (themselves deriving from the fusion of several richly labelled zymogen granule membranes) progressively lose their cholesterol to resemble ultimately the poorly labelled luminal membrane. If this interpretation is correct, then the question arises of the fate of the cholesterol removed from the exocytotic pocket. Again, this question may be tentatively answered on a purely morphological basis: after stimulated exocytotic release, one observes an accumulation of apical vesicles whose limiting membrane contains numerous filipin–cholesterol complexes (data not shown); in addition, there are sheets of membrane-like material in the acinar lumen (corresponding to the membrane blisters described by Borgese *et al.* (1979)), which are likewise rich in filipin–cholesterol complexes; these two membrane compartments may represent cholesterol-rich segments removed from the fused exocytotic pocket or from the luminal membrane locally enriched in cholesterol upon granule fusion, or from both.

† It is important to note that, under the same experimental conditions, the lateral membrane is richly labelled The sharp transition between the two patterns of filipin labelling (poorly labelled apical membrane and heavily labelled lateral membrane) appears to be partly abolished in acinar cells dissociated by trypsin–collagenase digestion.

‡ We interpret these clusters as representing coated membrane segments rather than 'undiluted' luminal membrane between particle-poor patches resulting from the incorporation of zymogen granule membrane, as suggested by De Camilli *et al.* (1976).

Description of plate 8

Figure 25. Pancreatic acinar cell stimulated and processed as described in figure 24. Aldehyde fixative containing filipin (300 μM) was injected into the duct system. Freeze–fracture of the apical pole showing a large membrane invagination such as that shown in figure 24 and interpreted as an exocytotic pocket. The protoplasmic leaflet of the pocket (EP(P)) is continuous with the protoplasmic leaflet of the luminal membrane (LM(P)), but only the pocket membrane appears labelled with f–c complexes. The labelling stops abruptly at the neck of the pocket merging into the luminal membrane. (Magn. × 48000.)

Figure 26. Pancreatic acinar cell stimulated and processed as described in figures 24 and 25. Freeze–fracture replica similar to that shown in figure 25 but revealing a difference in the pattern of filipin labelling of the exocytotic pocket (EP(P)). The transition between filipin-labelled and filipin-unlabelled membrane is no longer at the opening of the pocket on the luminal membrane (LM(P)) (cf. figure 25), but near the pocket's equator (dotted line). The sharpness of the transition is shown in the inset. (Magn. × 14000; inset, × 25000.)

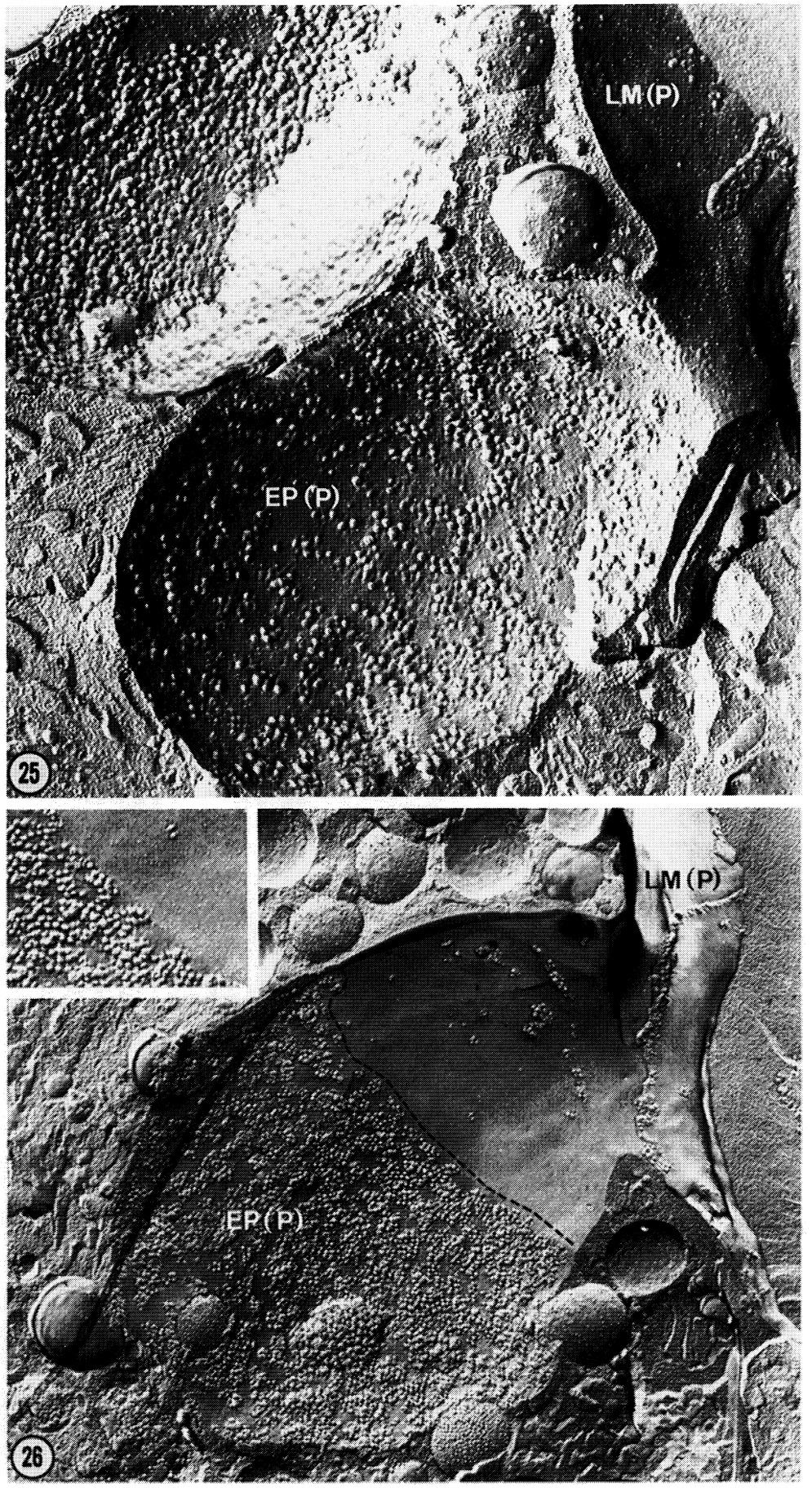

FIGURES 25 AND 26. For description see opposite.

(*Facing p.* 52)

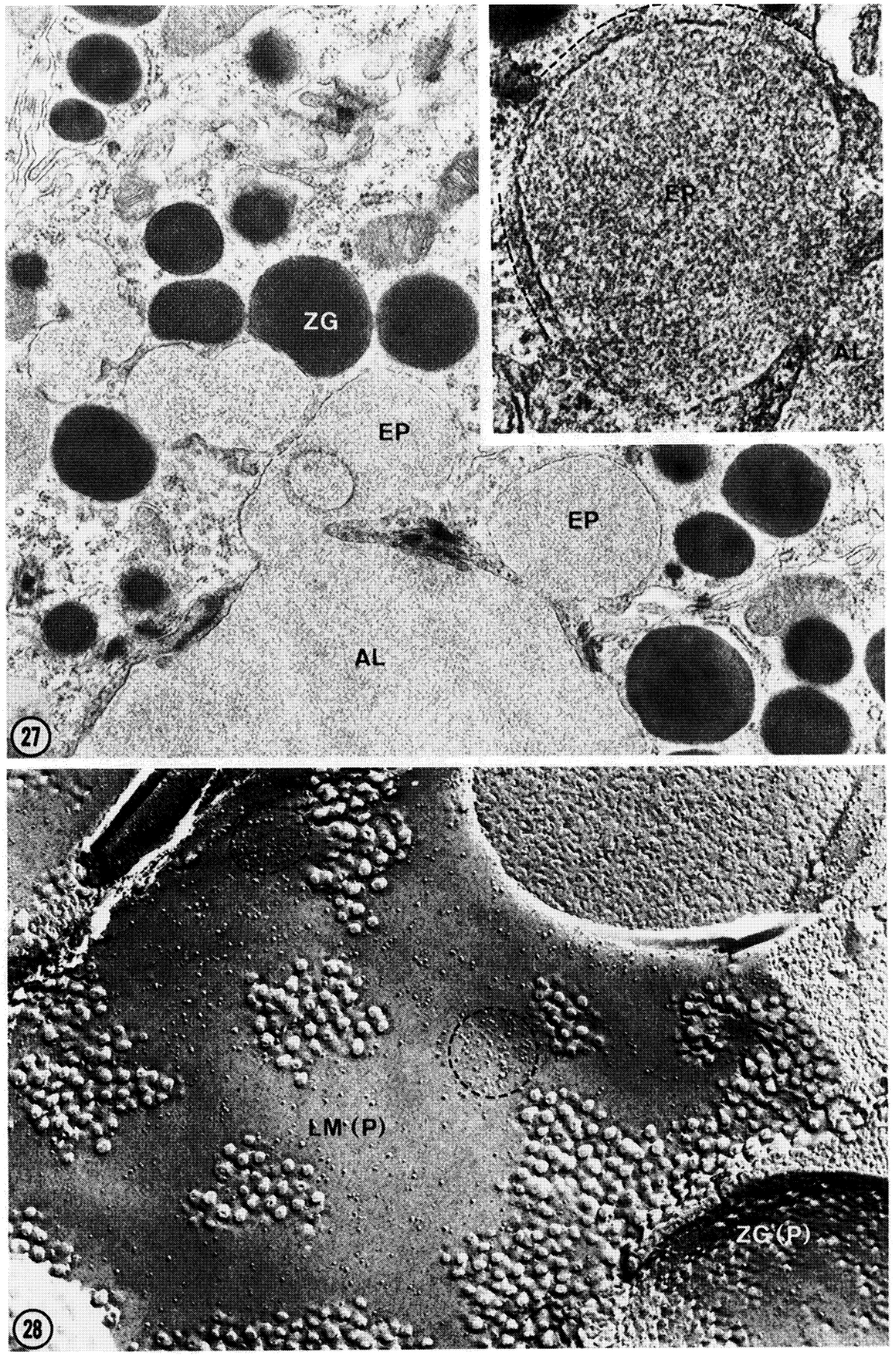

FIGURES 27 and 28. For description see opposite.

Description of plate 9

Figure 27. Parotid acinar cell stimulated for 5 min by an i.p. injection of isoprenalin (33 mg/kg) before aldehyde perfusion-fixation. Thin section of the apical pole showing the acinar lumen (AL) continuous with exocytotic pockets (EP) in the apical cytoplasm. The content of the exocytotic pocket and of the acinar lumen is markedly less dense than that of zymogen granules (ZG). The inset shows that the limiting membrane of the pocket (EP) opened at the acinar lumen (AL) is associated with a band of microfilamentous material (indicated by a dotted line). (Magn. × 20000; inset, × 45000.)

Figure 28. Parotid acinar cell stimulated and processed as described in figure 27. Filipin treatment was carried out as detailed in figure 23. Freeze–fracture replica of the apical pole showing a large portion of the protoplasmic leaflet of the luminal membrane (LM(P)). This membrane face contains patches of f–c complexes and clusters of intramembrane particles (dotted lines). Such clusters may represent coated regions of the luminal membrane. In the lower right corner, a small portion of richly labelled zymogen granule membrane (ZG(P)) is detectable. (Magn. × 63000.)

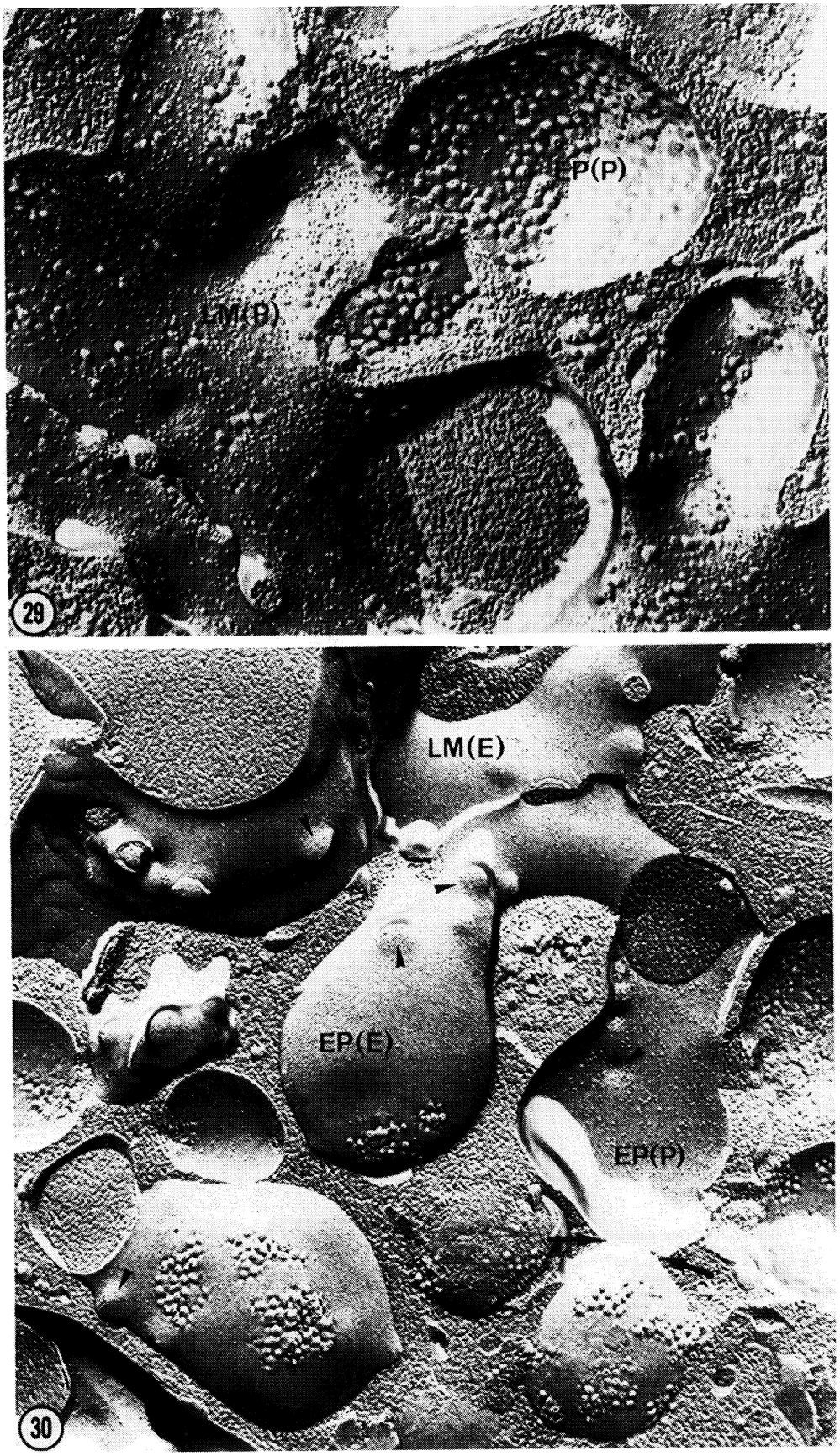

FIGURES 29 AND 30. For description see opposite.

At this point, it must be stressed that the proposed interpretations take into account solely the observed distribution of particles and filipin–cholesterol complexes; moreover, they are based on the assumption that the differences observed reflect only underlying differences in the protein and cholesterol content of the membrane, an assumption that is incapable of proof at present. In spite of these restrictions, we nevertheless feel that our studies with the use of intramembrane particles as protein markers and filipin as a probe for cholesterol distribution represent a useful framework to further explore membrane interactions during secretion.

Supported by the Swiss National Science Foundation, grant no. 3.668.80. We thank M. Bernard, P. Fruleux and P. Sors for technical assistance and Isabelle Bernard for secretarial work.

References (Orci *et al.*)

Branton, D. 1969 Membrane structure. *A. Rev. Pl. Physiol.* **20**, 209–238.

Borgese, N., De Camilli, P., Tanaka, Y. & Meldolesi, J. 1979 Membrane interactions in secretory cell systems. In *Secretory mechanisms* (*Symp. Soc. exp. Biol.* no. 33), (ed. C. R. Hopkins & C. J. Duncan), pp. 117–144. Cambridge University Press.

Chandler, D. E. & Heuser, J. 1979 Membrane fusion during secretion. Cortical granule exocytosis in sea urchin eggs as studied by quick-freezing and freeze–fracture. *J. Cell Biol.* **83**, 91–108.

Chandler, D. E. & Heuser, J. E. 1980 Arrest of membrane fusion events in mast cells by quick-freezing. *J. Cell Biol.* **86**, 666–674.

Deamer, D. W. 1977 The relation of membrane ultrastructure to membrane function. In *Mammalian cell membranes*, vol. 4 (ed. G. A. Jamieson & D. M. Robinson), pp. 1–31. London: Butterworth.

De Camilli, P., Peluchetti, D. & Meldolesi, J. 1974 Structural difference between luminal and lateral plasmalemma in pancreatic acinar cells. *Nature, Lond.* **248**, 245–246.

De Camilli, P., Peluchetti, D. & Meldolesi, J. 1976 Dynamic changes of the luminal plasmalemma in stimulated parotid acinar cells. A freeze–fracture study. *J. Cell Biol.* **70** 59–74.

De Kruijff, B., Gerritsen, W. J., Oerlemans, A., Demel, R. A. & Van Deenen, L. L. M. 1974 Polyene antibiotic–sterol interactions in membranes of *Acholeplasma laidlawii* cells and lecithin liposomes. I. Specificity of the membrane permeability changes induced by the polyene antibiotics. *Biochim. biophys. Acta* **339**, 30–43.

Elias, P. M., Friend, D. S. & Goerke, J. 1979 Membrane sterol heterogeneity. Freeze–fracture detection with saponins and filipin. *J. Histochem. Cytochem.* **27**, 1247–1260.

Friend, D. S. 1980 Freeze–fracture alterations in guinea pig sperm membranes preceding gamete fusion. In *Membrane–membrane interactions* (ed. N. B. Gilula), pp. 153–165. New York: Raven Press.

Lagunoff, D. 1973 Membrane fusion during mast cell secretion. *J. Cell Biol.* **57**, 252–259.

Lawson, D., Raff, M. C., Gomperts, B., Fewtrell, C. & Gilula, N. B. 1977 Molecular events during membrane fusion. A study of exocytosis in rat peritoneal mast cells. *J. Cell Biol.* **72**, 242.

McNutt, N. S. 1977 Freeze–fracture techniques and applications to the structural analysis of the mammalian plasma membrane. In *Dynamic aspects of cell surface organization* (*Cell Surface Reviews*, vol. 3) (ed. G. Poste & G. L. Nicolson), pp. 75–126. Amsterdam: Elsevier/North-Holland.

Meldolesi, J., Borgese, N., De Camilli, P. & Ceccarelli, B. 1978 Cytoplasmic membranes and secretory process. In *Membrane fusion* (*Cell Surface Reviews*, vol. 5) (ed. G. Poste and G. L. Nicolson), pp. 509–627. Amsterdam: Elsevier/North-Holland.

Description of plate 10

Figures 29 and 30. Parotid acinar cells stimulated and processed as described in figure 27. Filipin treatment was carried out as detailed in figure 23. Freeze–fracture replicas of the apical pole showing the luminal membrane continuous with invaginated membrane segments of exocytotic pockets (cf. figure 27). Figure 29 shows sparse filipin labelling of the protoplasmic leaflet of the luminal membrane (LM(P)), contrasting with abundant labelling of the exocytotic pocket (EP(P)). Figure 30 shows a lack of f–c complexes in the luminal membrane (LM(E)) and in two directly continuous exocytotic pocket membranes (EP(E) and EP(P)), except in the bottom part of the pocket (EP(E)). F–c complexes also appear on a membrane face apparently fused (arrows) with an exocytotic pocket (EP(P)). Such images and those shown in figures 25 and 26 suggest that the zymogen granule membrane progressively loses its ability to bind filipin (cholesterol removal?) upon fusion with the cholesterol-poor luminal membranes. Several circular bulges (E-leaflet) or depressions (P-leaflet) (arrowheads) represent coated pits. (Magns: figure 29, × 50000; figure 30, × 33000.)

Montesano, R., Perrelet, A., Vassalli, P. & Orci, L. 1979 Absence of filipin–sterol complexes from large coated pits on the surface of culture cells. *Proc. natn. Acad. Sci. U.S.A.* **76**, 6391–6395.

Montesano, R., Vassalli, P., Perrelet, A. & Orci, L. 1980 Distribution of filipin–cholesterol complexes at sites of exocytosis. A freeze–fracture study of degranulating mast cells. *Cell Biol. int. Rep.* **4**, 975–984.

Norman, A. W., Demel, R. A., De Kruijff, B. & Van Deenen, L. L. M. 1972 Studies on the biological properties of polyene antibiotics. Evidence for the direct interaction of filipin with cholesterol. *J. biol. Chem.* **247**, 1918–1929.

Norman, A. W., Spielvogel, A. M. & Wong, R. G. 1976 Polyene antibiotic–sterol interaction. *Adv. Lipid Res.* **14**, 127–170.

Orci, L. 1974 A portrait of the pancreatic β-cell. *Diabetologia* **10**, 163–187.

Orci, L., Montesano, R. & Brown, D. 1980 Heterogeneity of toad bladder granular cell luminal membranes. Distribution of filipin–sterol complexes in freeze–fracture. *Biochim. biophys. Acta* **601**, 443–452.

Orci, L., Montesano, R., Meda, P., Malaisse-Lagae, F., Brown, D., Perrelet, A. & Vassalli, P. 1981 Heterogeneous distribution of filipin–cholesterol complexes across the cisternae of the Golgi apparatus. *Proc. natn. Acad. Sci. U.S.A.* **78**, 293–297.

Orci, L. & Perrelet, A. 1978 Ultrastructural aspects of exocytotic membrane fusion. In *Membrane fusion (Cell Surface Reviews,* vol. 5) (ed. G. Poste & G. L. Nicolson), pp. 629–656. Amsterdam: Elsevier/North-Holland.

Orci, L., Perrelet, A. & Friend, D. S. 1977 Freeze–fracture of membrane fusions during exocytosis in pancreatic β-cells. *J. Cell Biol.* **75**, 23–30.

Palade, G. 1975 Intracellular aspects of the process of protein synthesis. *Science, Wash.* **189**, 347–358.

Palade, G. & Bruns, R. R. 1968 Structural modulations of plasmalemmal vesicles. *J. Cell Biol.* **37**, 633–649.

Plattner, H. 1981 Membrane behaviour during exocytosis. *Cell Biol. int. Rep.* **5**, 435–459.

Robertson, J. D. 1959 The ultrastructure of cell membranes and their derivatives. *Biochem. Soc. Symp.* **16**, 3–43.

Robinson, J. M. & Karnovsky, M. J. 1980 Evaluation of the antibiotic filipin as a cytochemical probe for membrane cholesterol. *J. Histochem. Cytochem.* **28**, 161–168.

Singer, S. J. & Nicolson, G. L. 1972 The fluid mosaic model of the structure of cell membranes. *Science, Wash.* **175**, 720–731.

Tartakoff, A. M. 1980 The Golgi complex: crossroads for vesicular traffic. *Int. Rev. exp. Path.* **22**, 227–251.

Tillack, T. W. & Kinsky, S. C. 1973 A freeze–etch study of the effects of filipin on liposomes and human erythrocyte membranes. *Biochim. biophys. Acta* **323**, 43–54.

Verkleij, A. J., De Kruijff, B., Gerritsen, W. J., Demel, R. A., Van Deenen, L. L. M. & Ververgaert, P. H. J. 1973 Freeze–etch electron microscopy of erythrocytes, *Acholeplasma laidlawii* cells and liposomal membranes after the action of filipin and amphotericin B. *Biochim. biophys. Acta* **291**, 577–581.

Whaley, W. G. & Dauwalder, M. 1979 The Golgi apparatus, the plasma membrane and functional integration. *Int. Rev. Cytol.* **58**, 199–245.

Yu, J. & Branton, D. 1976 Reconstitution of intramembrane particles in recombinants of erythrocyte protein Band 3 and lipid: effect of spectrin–actin association. *Proc. natn. Acad. Sci. U.S.A.* **73**, 3891–3895.

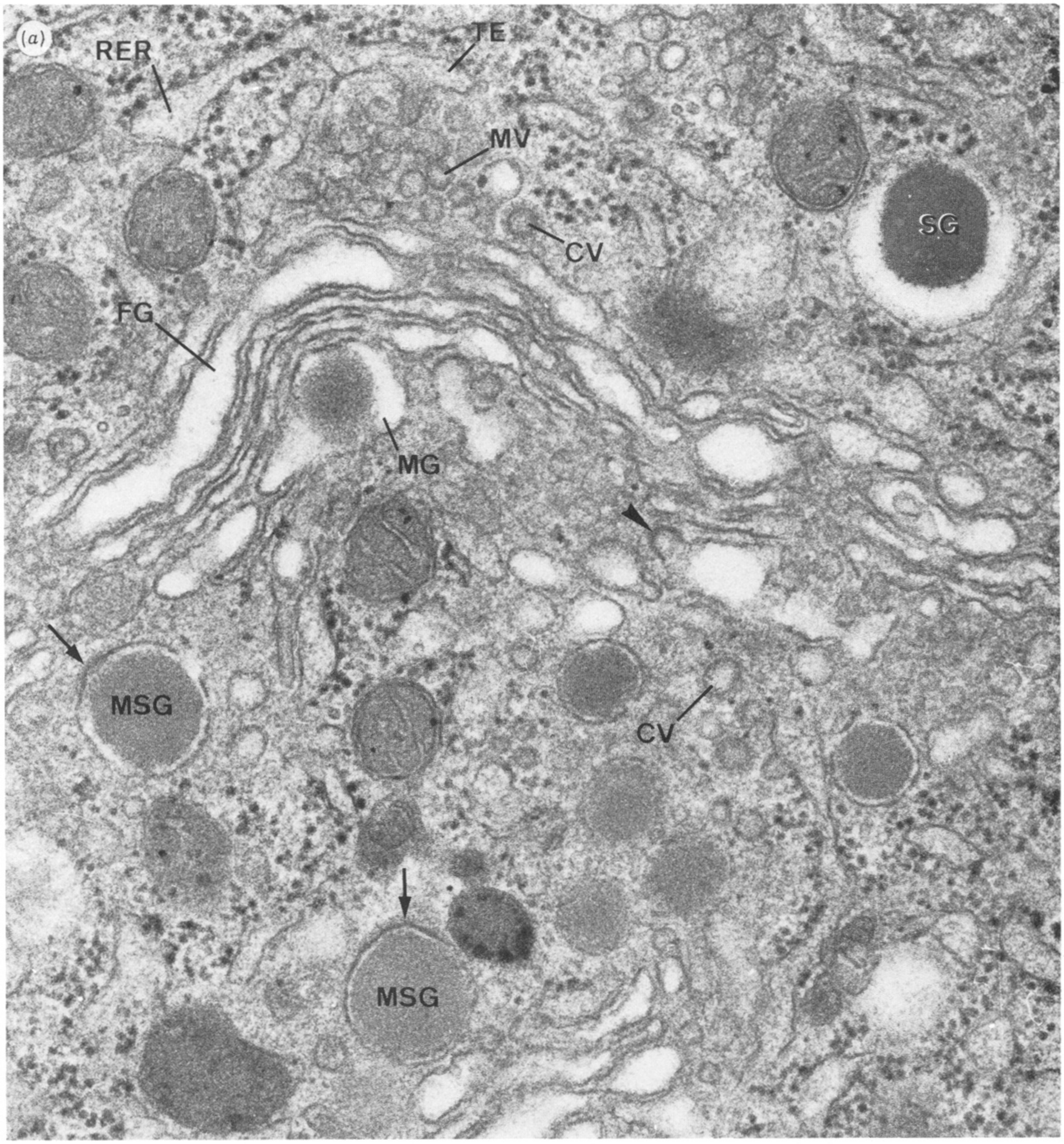

FIGURE 1. For description see opposite.

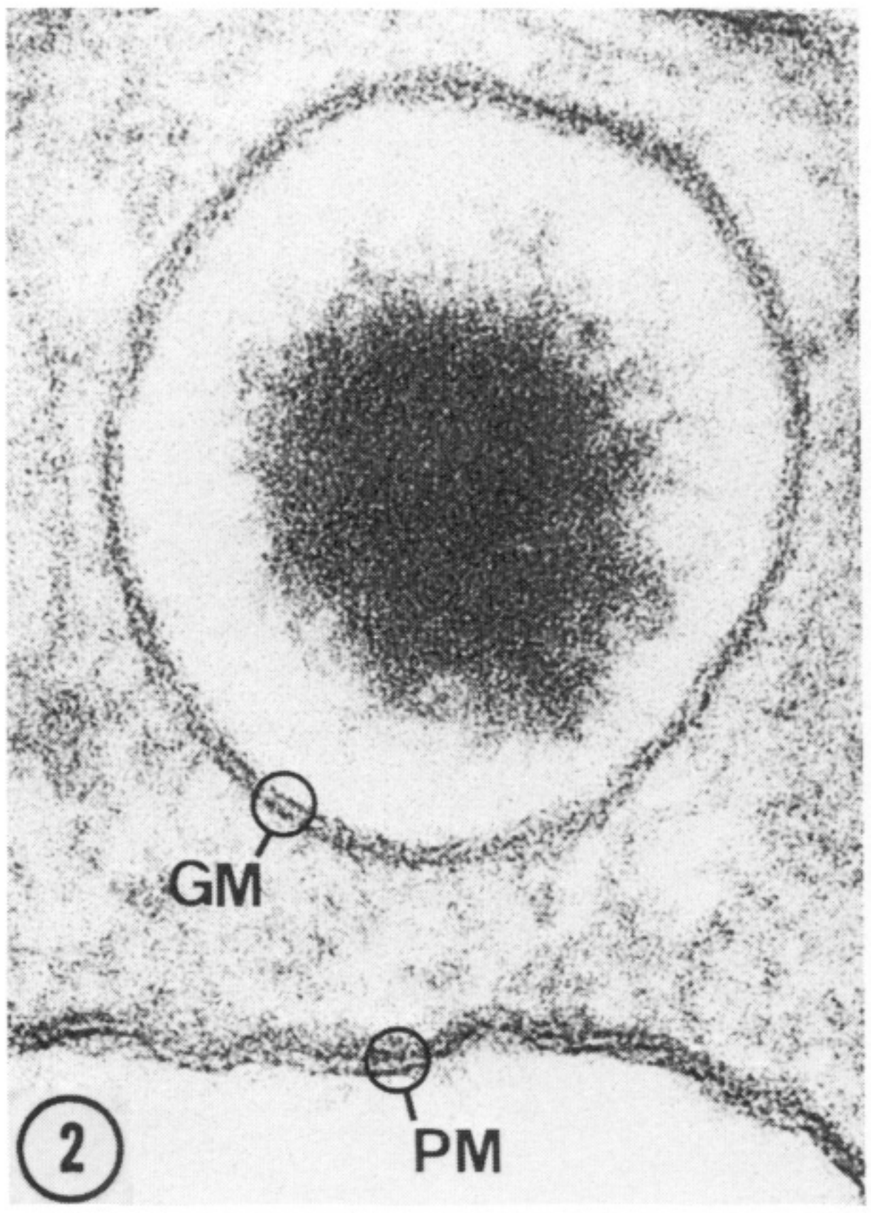

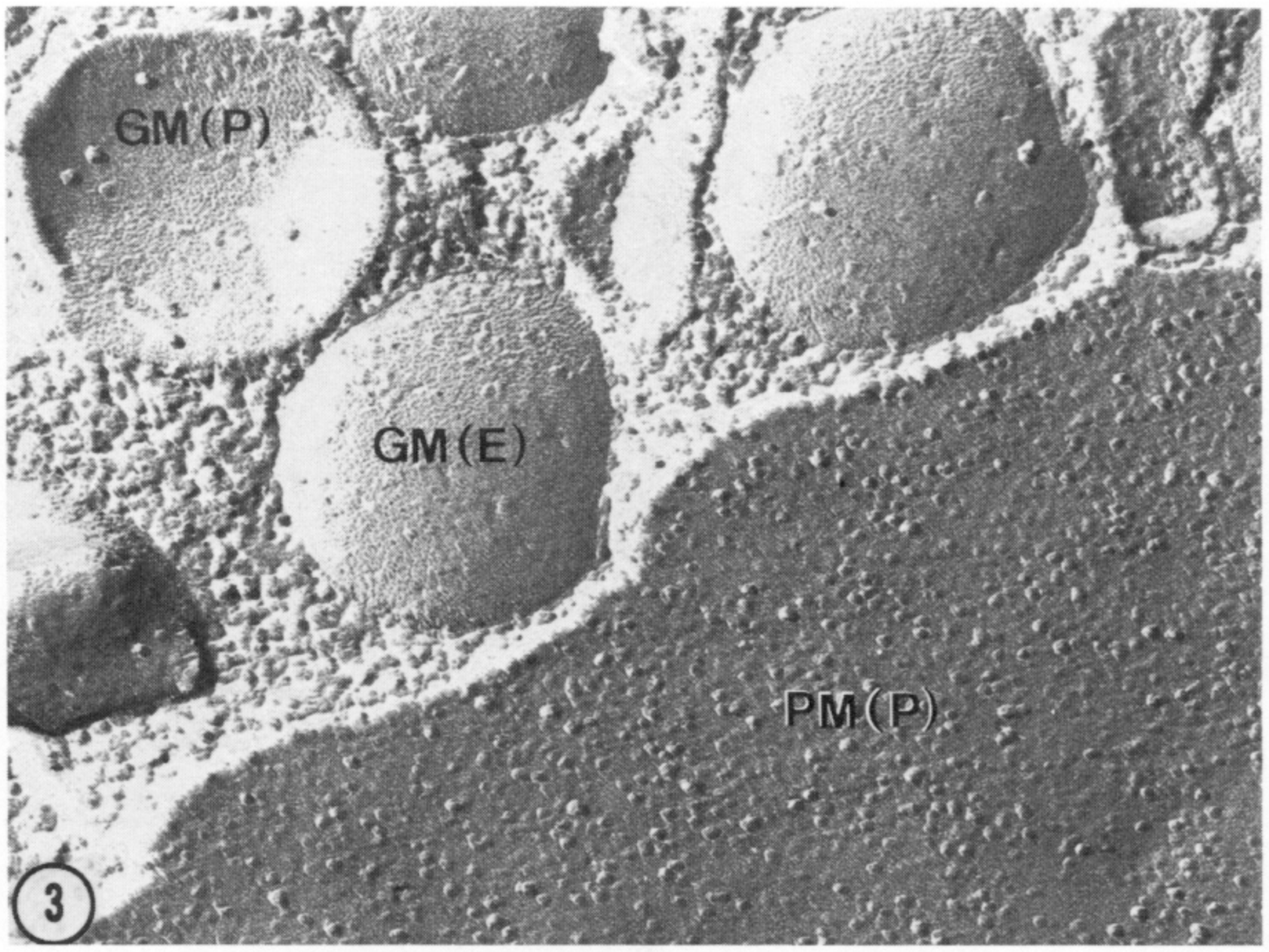

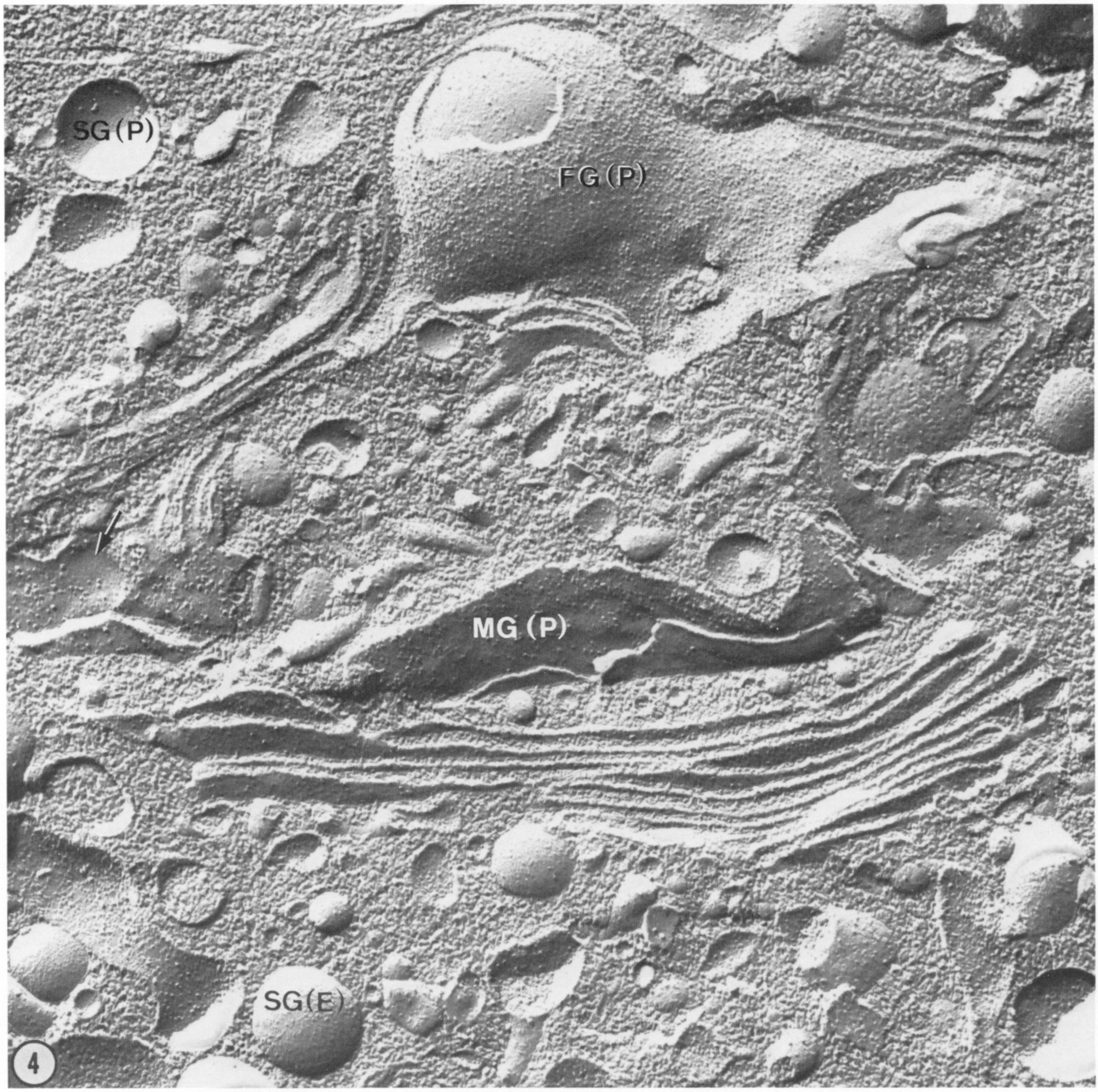

FIGURES 2–4. For description see opposite.

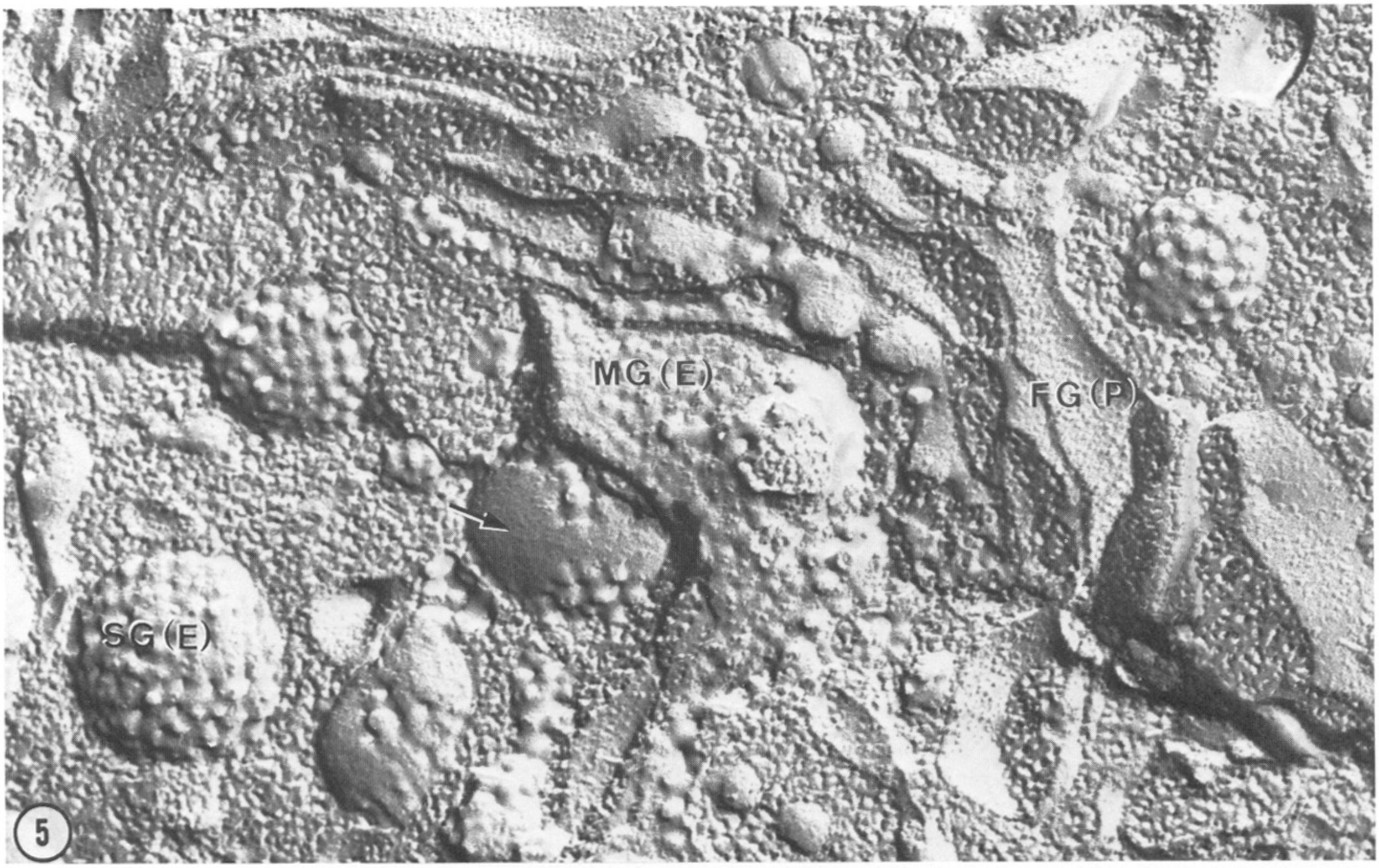

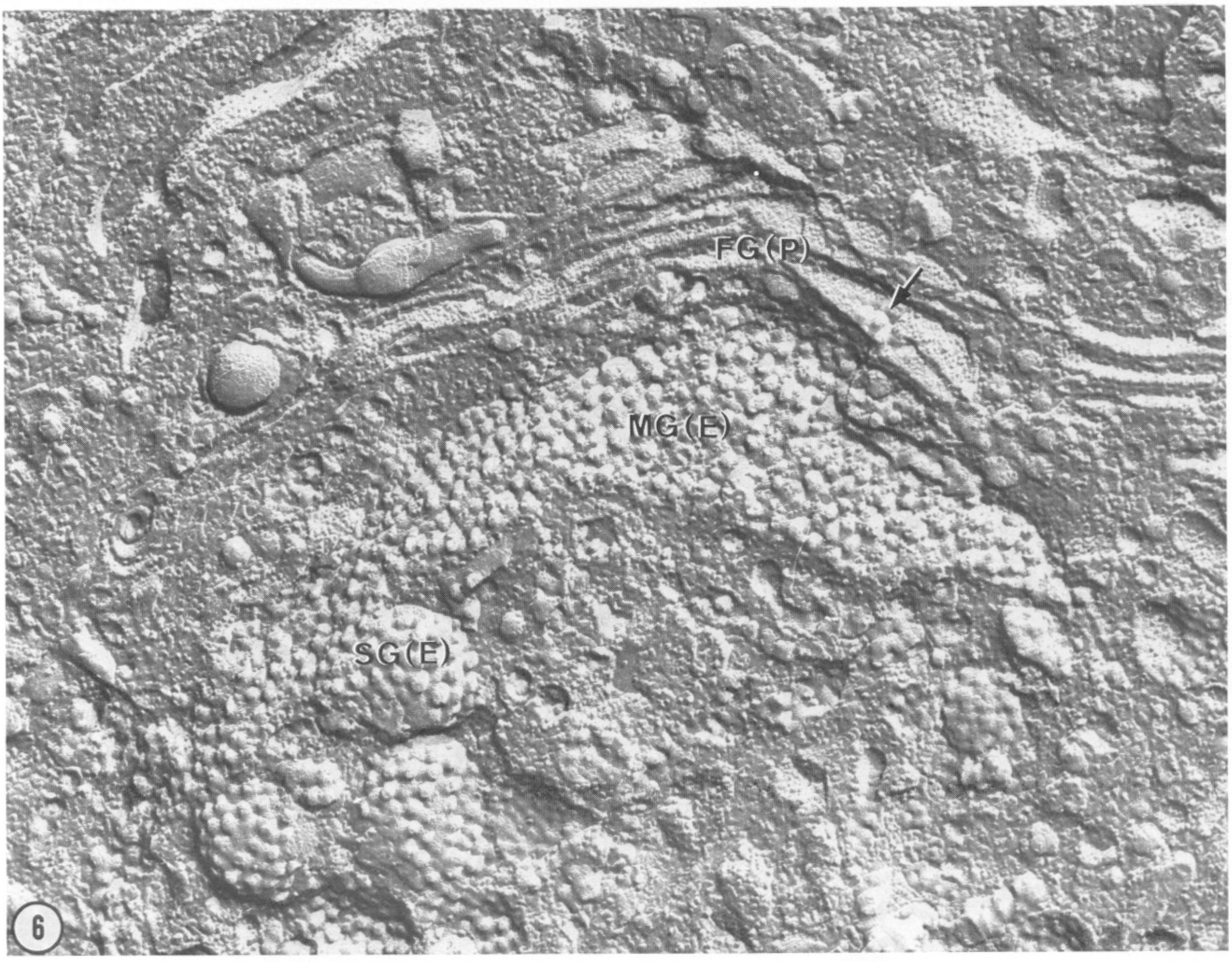

FIGURES 5 AND 6. For description see opposite.

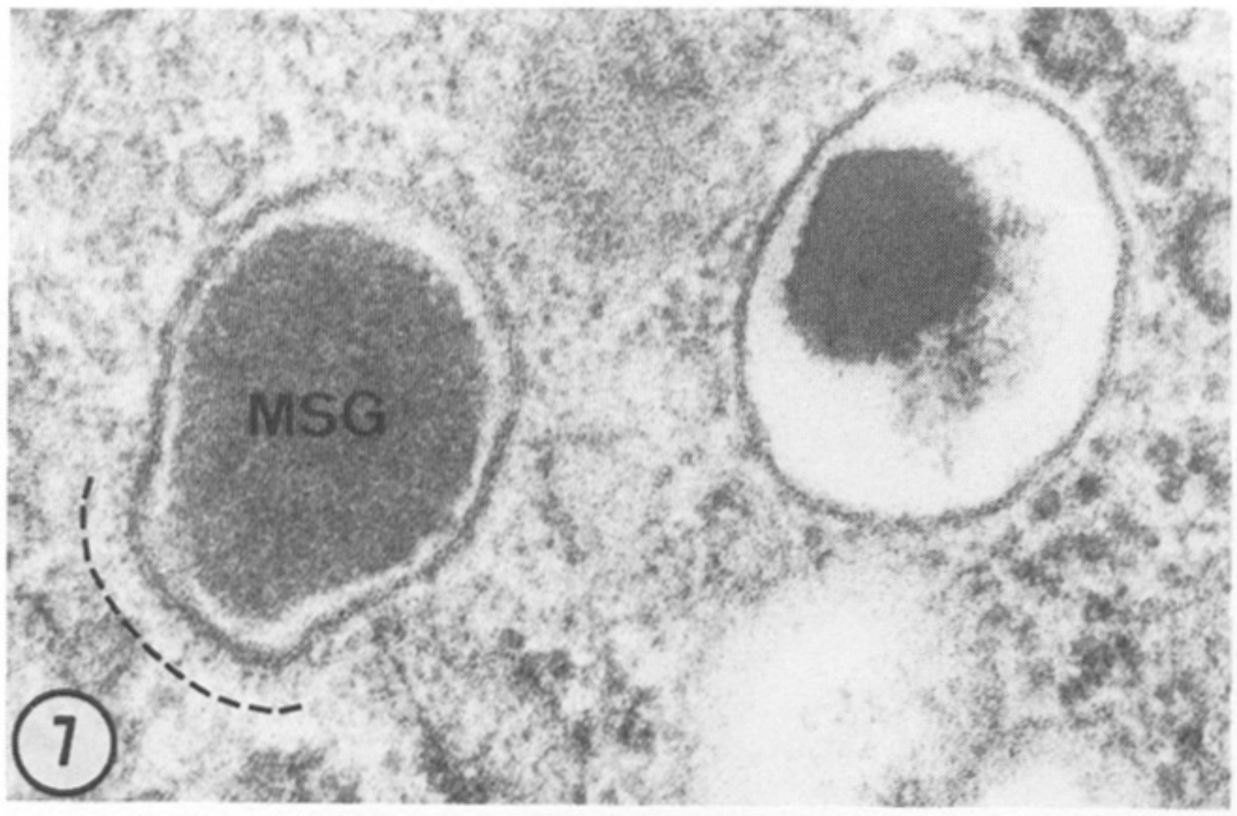

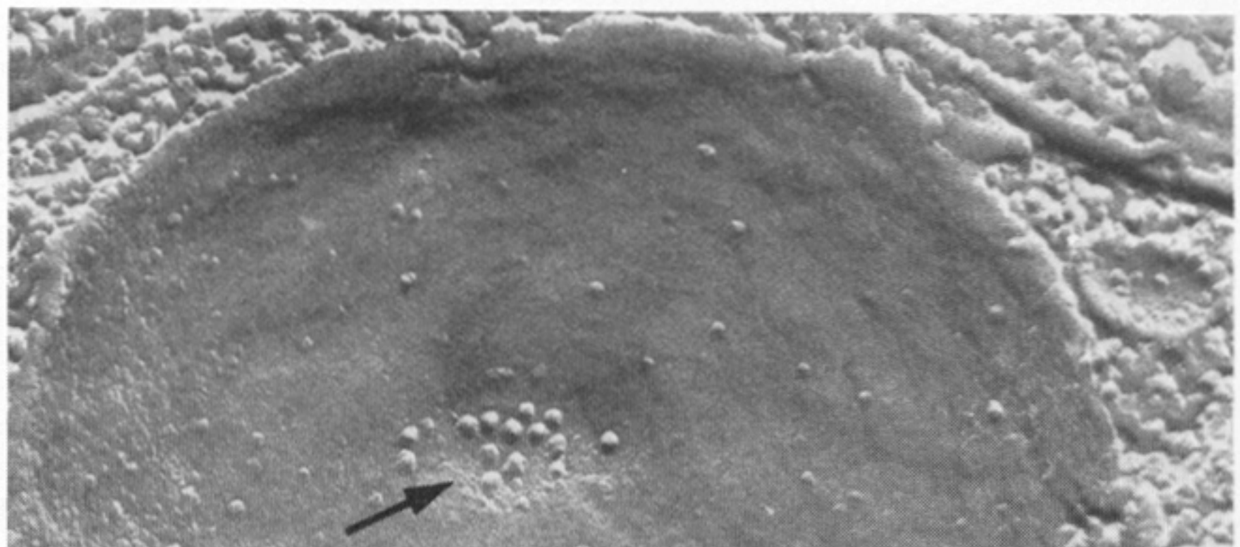

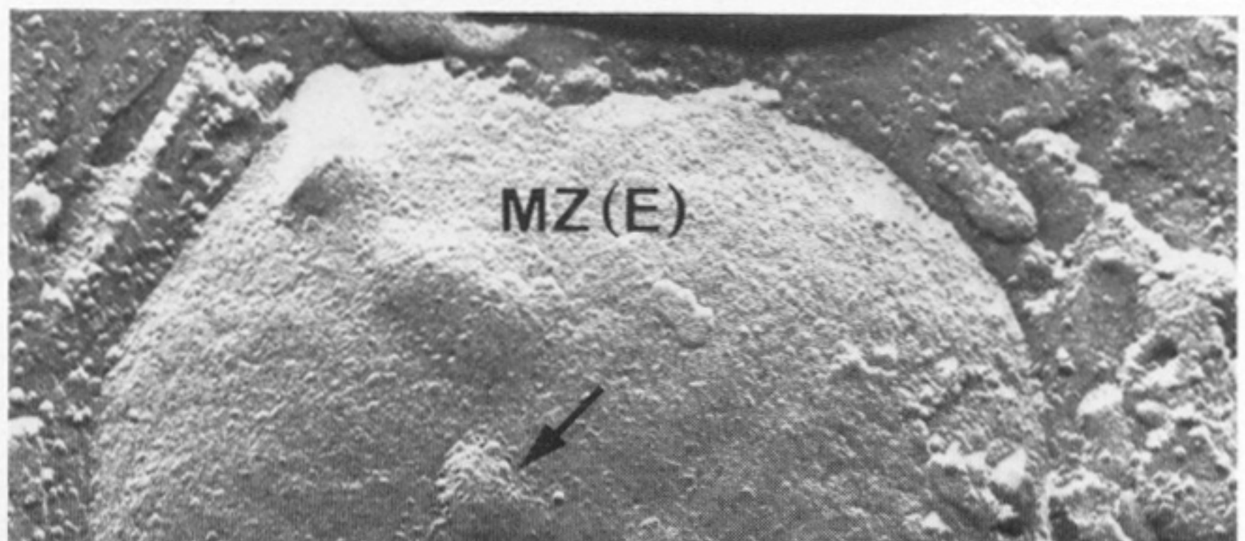

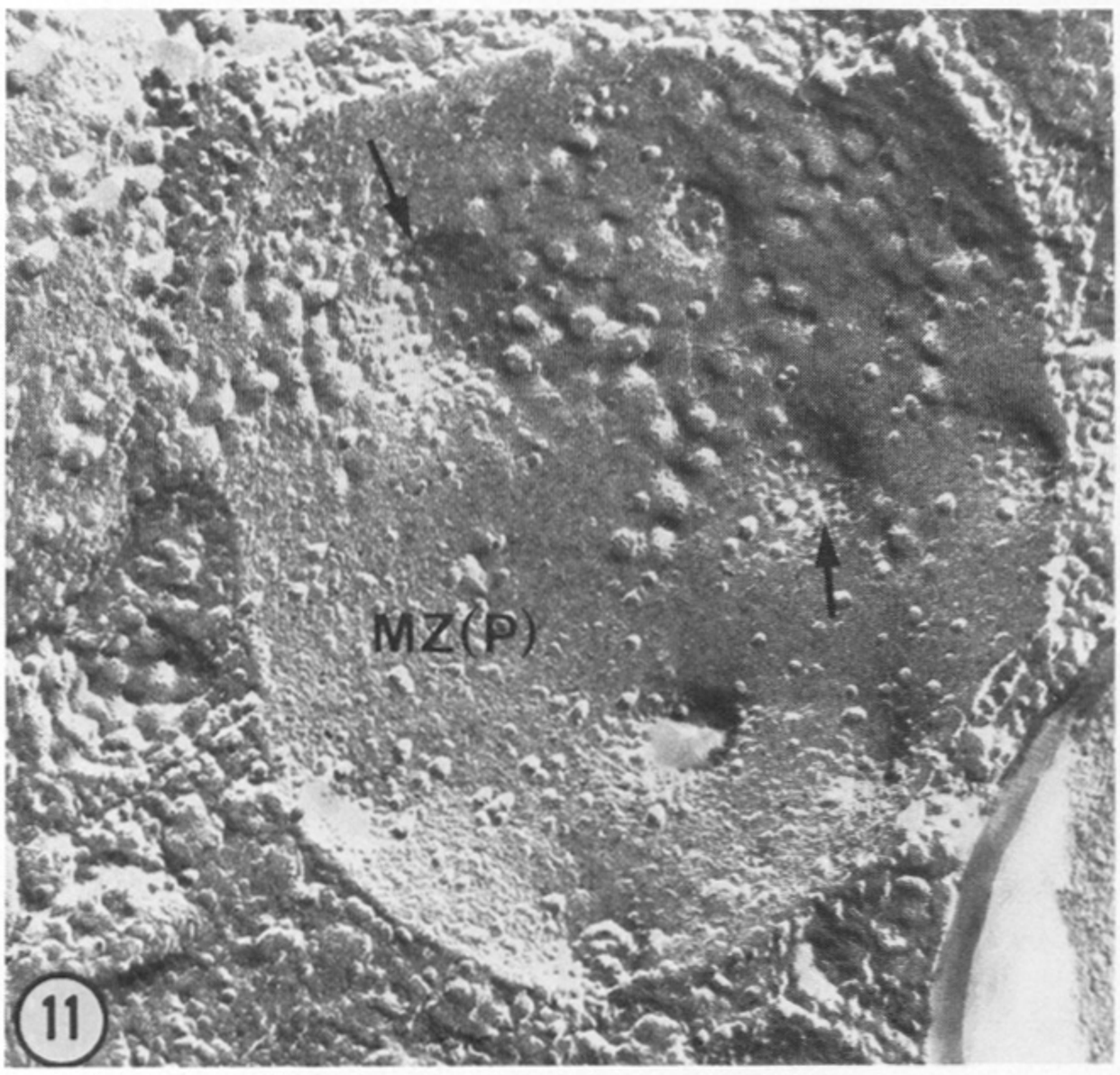

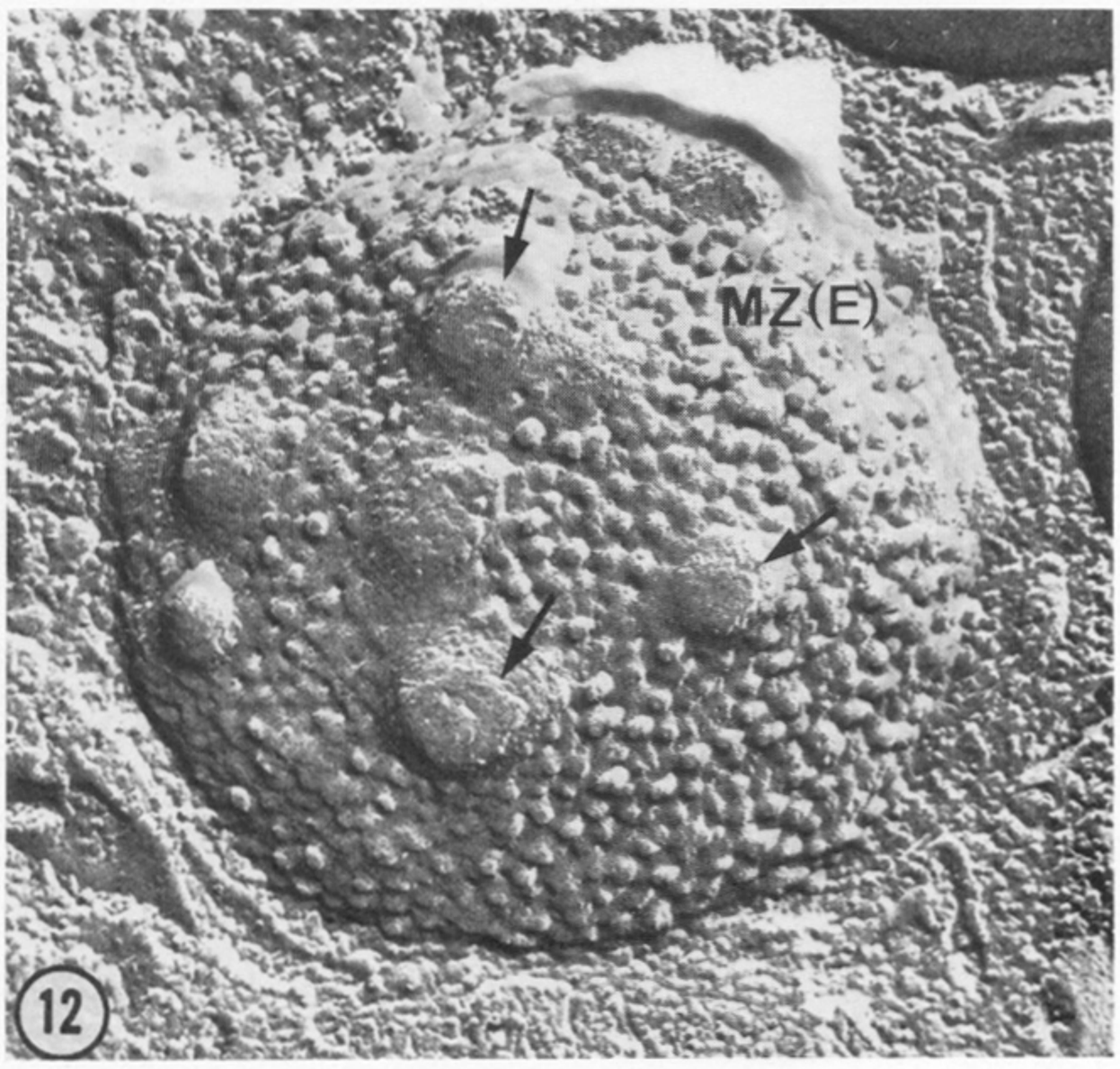

FIGURES 7–12. For description see opposite.

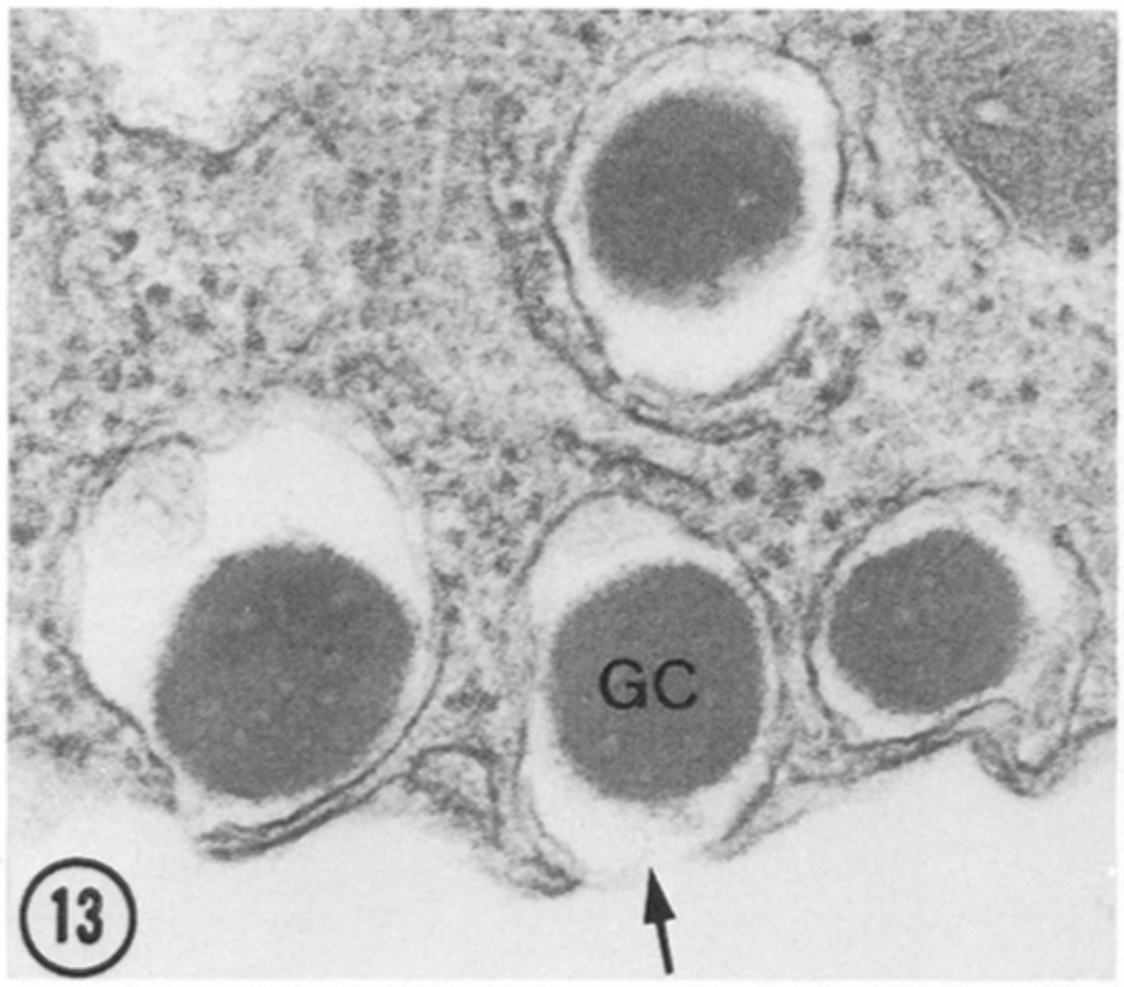

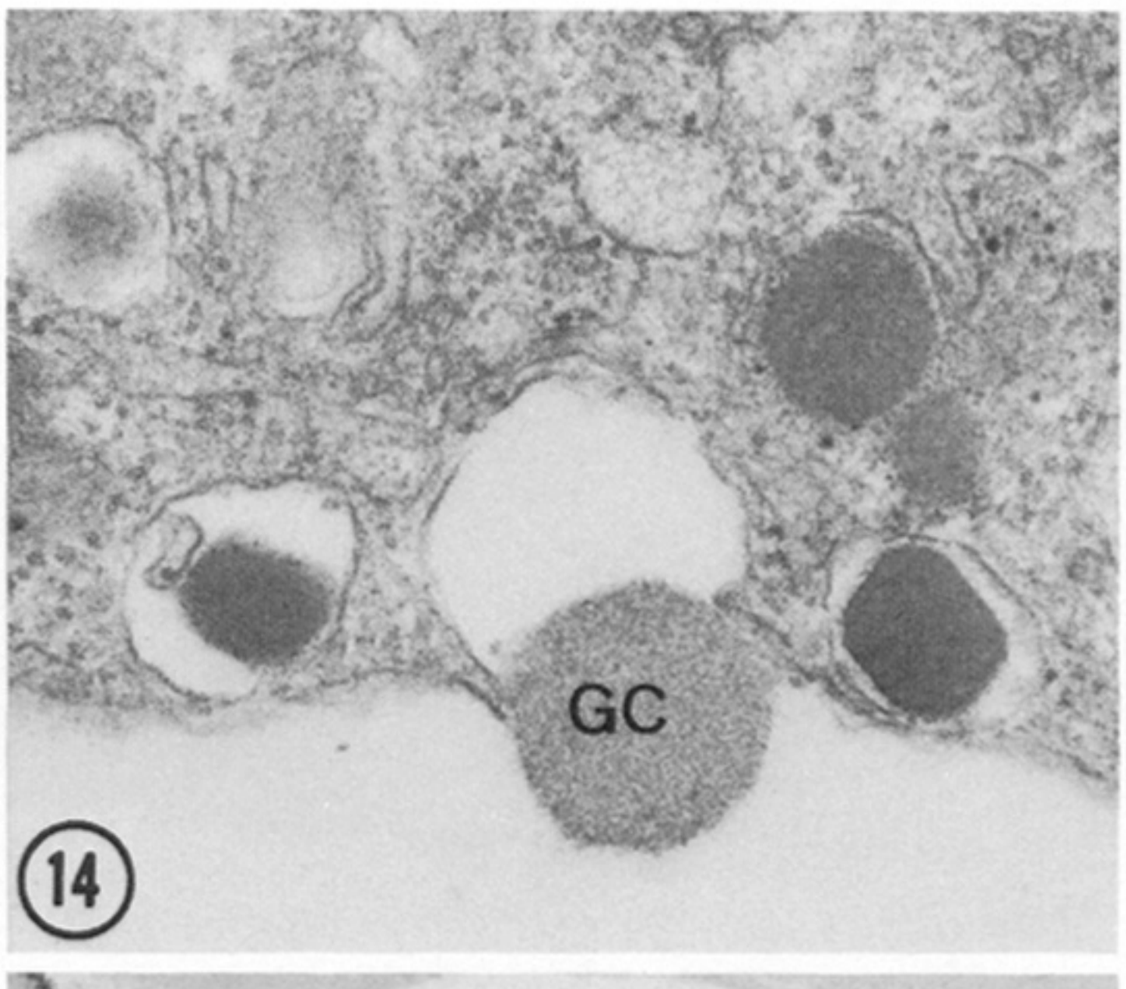

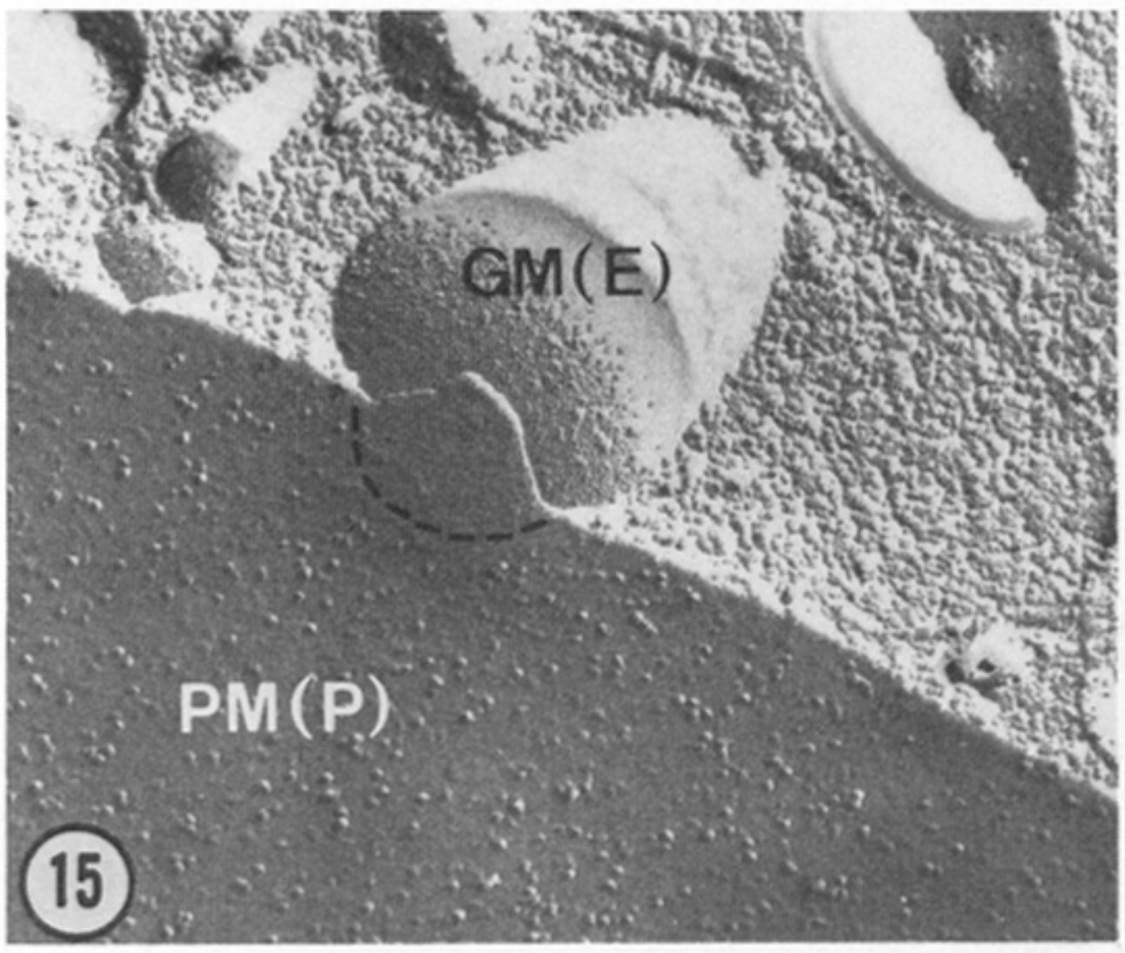

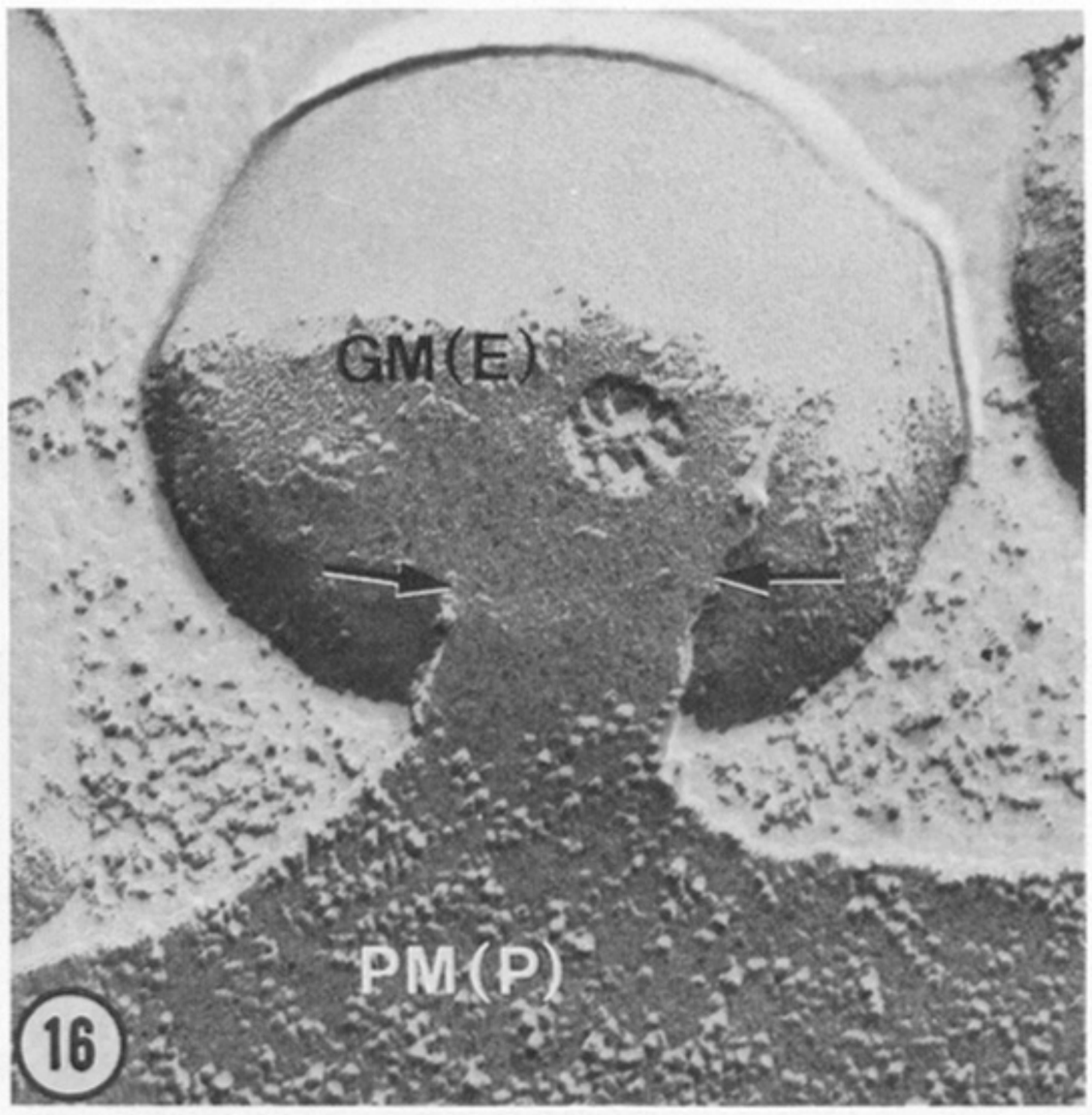

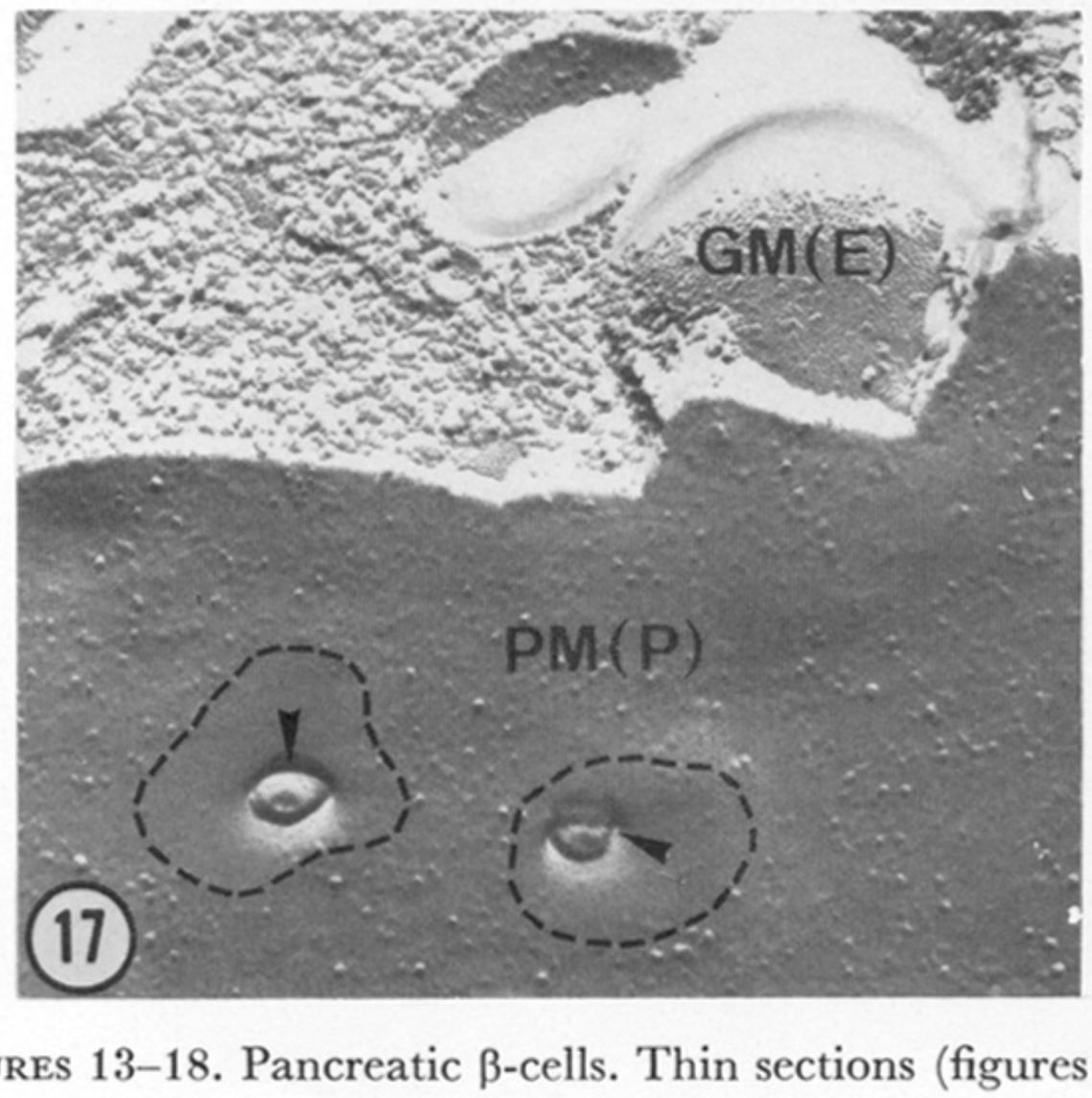

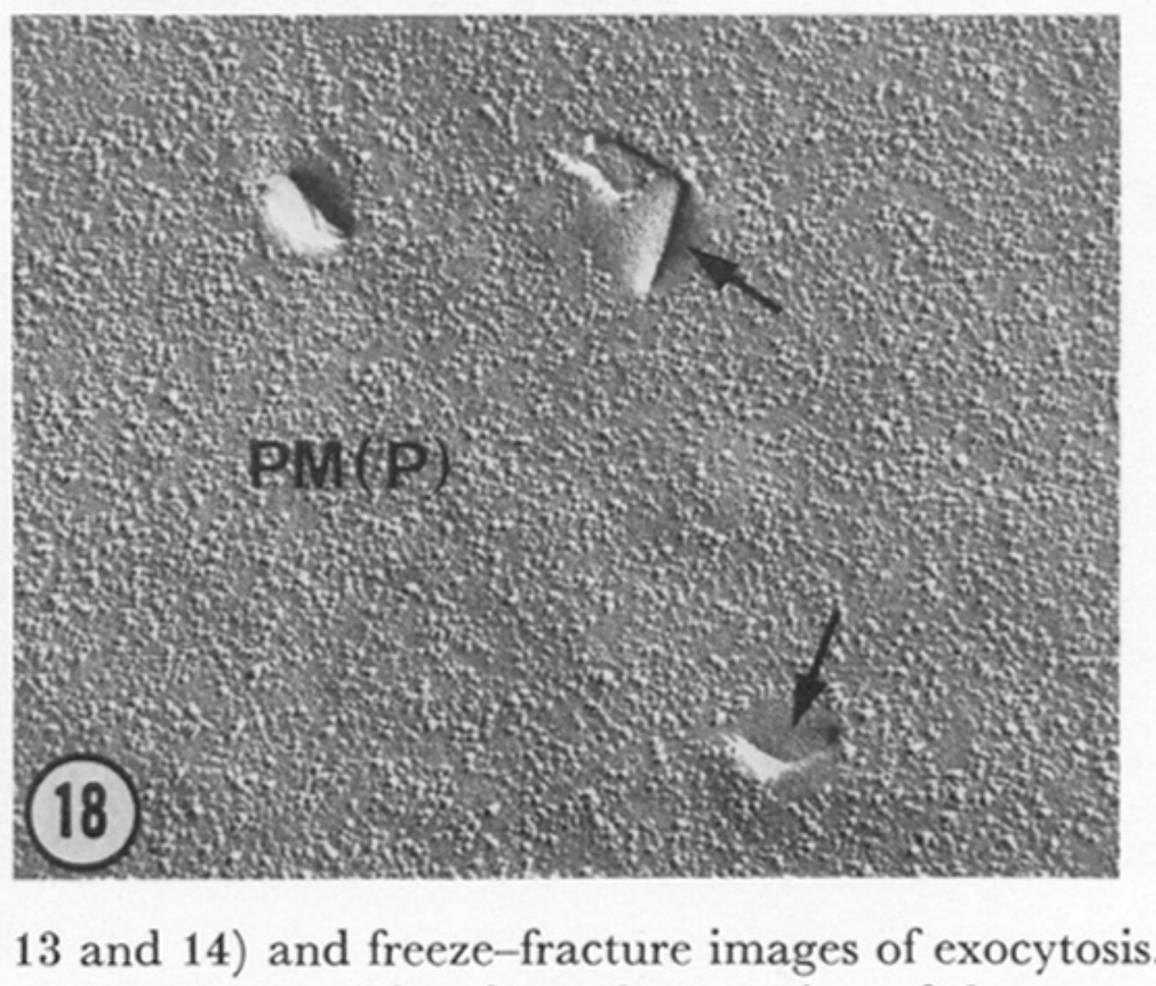

FIGURES 13–18. Pancreatic β-cells. Thin sections (figures 13 and 14) and freeze–fracture images of exocytosis. In thin section, exocytosis appears as a plasma membrane pocket resulting from the merging of the secretory granule membrane with the plasma membrane, exposing the granule core (GC) to the extracellular space. In freeze–fracture specimens of aldehyde-fixed, glycerol-impregnated cells, the pre-fusion stage (figure 15) appears as a particle-free patch (dotted line) in the cytoplasmic leaflet of the plasma membrane (PM(P)) overlying the poorly particulated secretory granule membrane (GM(E)). Figure 16 shows the merging (at the arrows) of the two membranes (GM(E), PM(P)) in a particle-free area; figures 17 and 18 show post-fusion stages in the cytoplasmic leaflet of the plasma membrane (PM(P)). These consist of particle-free patches of various shapes (dotted lines in figure 17; arrow in figure 18). In figure 17, the bulging mass in the particle-free area probably represents extruded granule core material (arrowhead). (Magns: figure 13, ×49000; figure 14, ×43000; figure 15, ×71000; figure 16, ×81000; figure 17, ×67000; figure 18, ×44000.) (Figures 13–15, 17 and 18 by courtesy of *J. Cell Biol.* (Orci *et al.* 1977); figure 16 by courtesy of Elsevier/North-Holland (Orci & Perrelet 1978).)

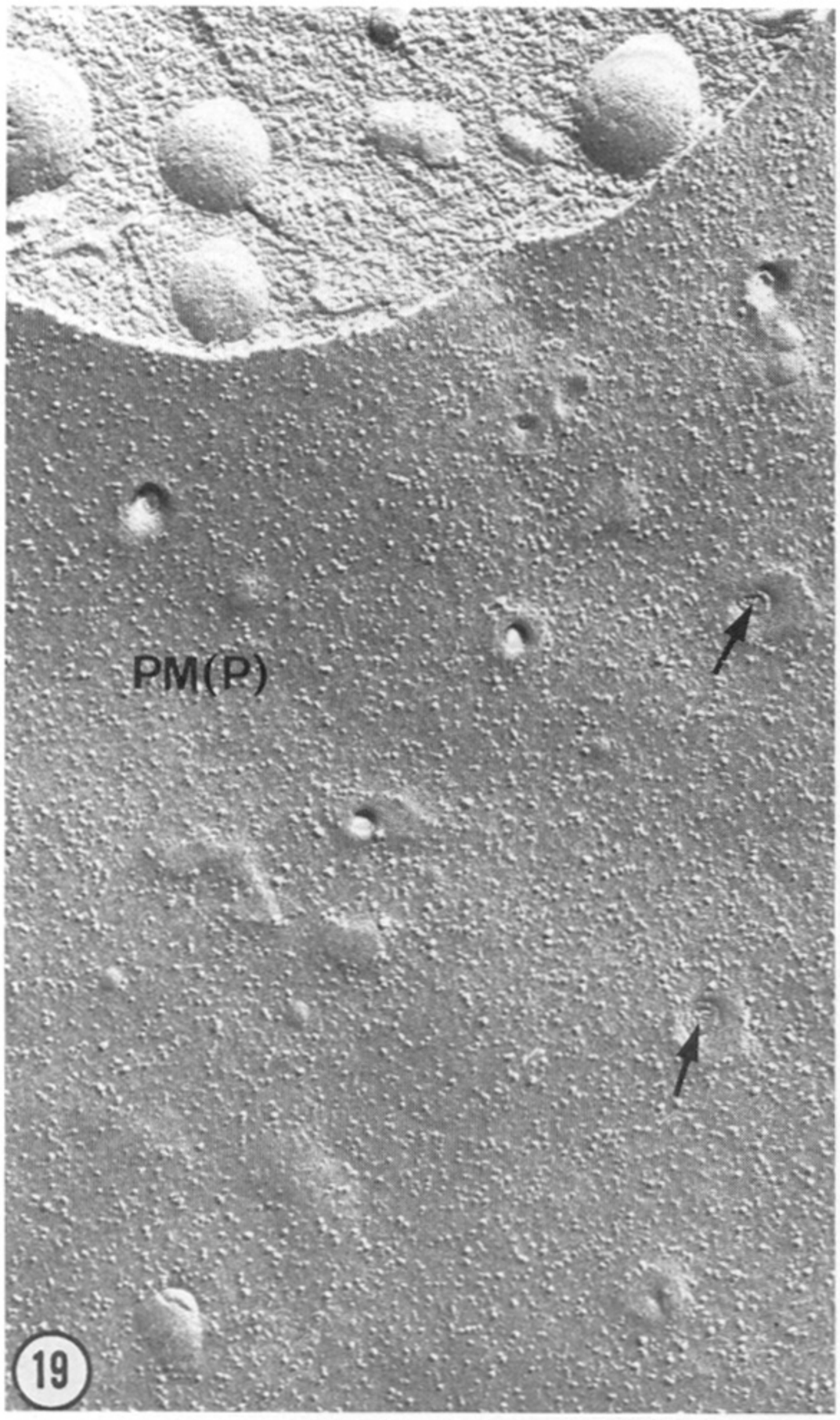

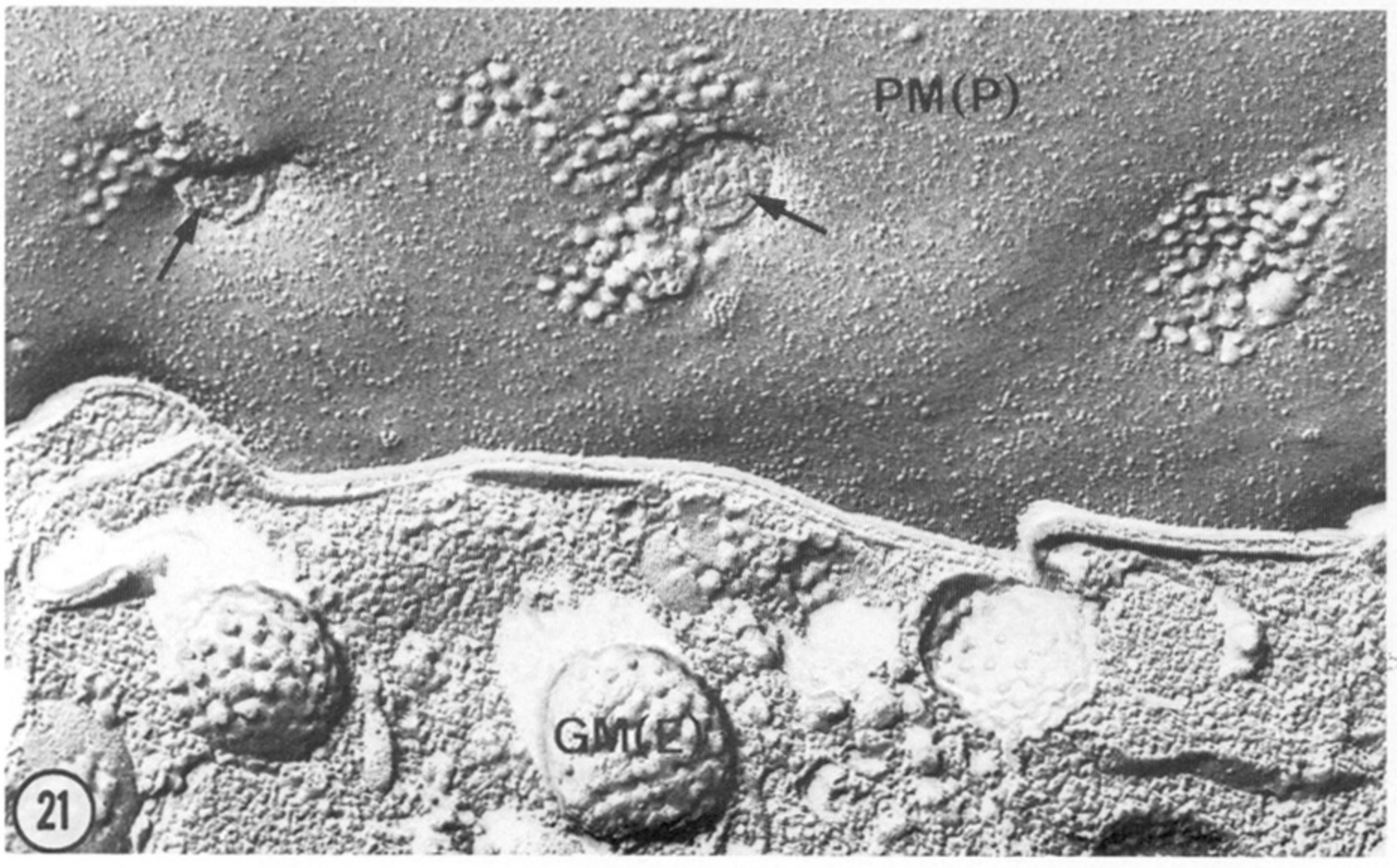

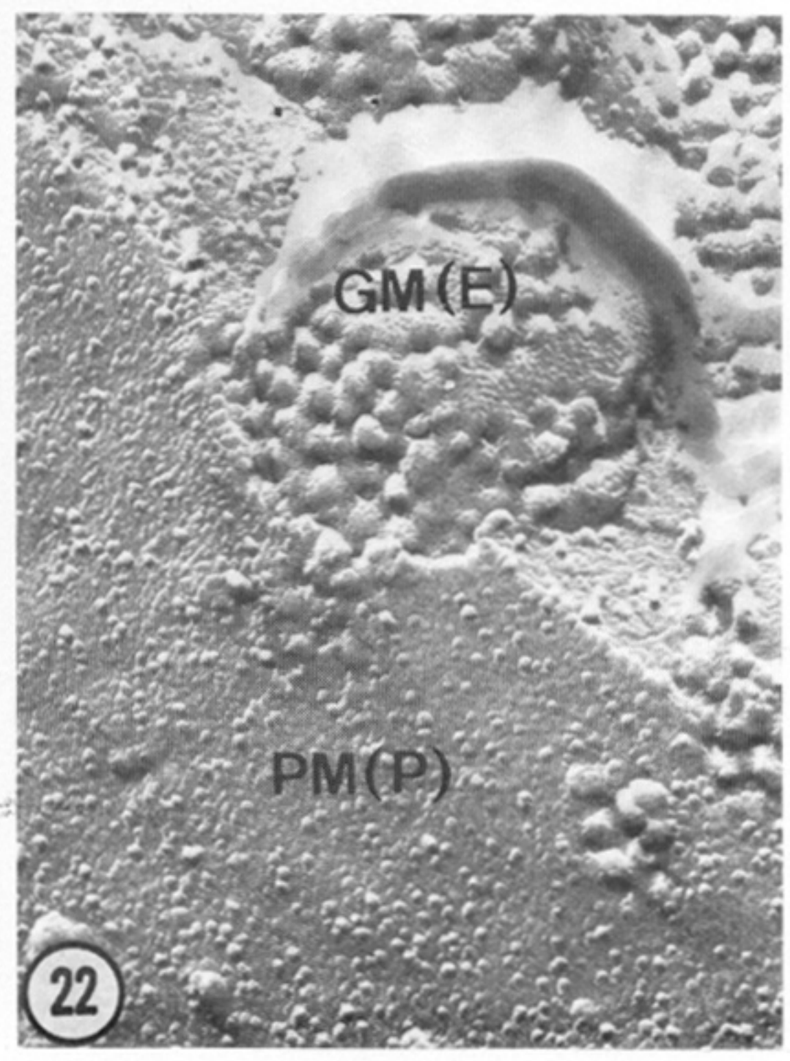

FIGURES 19–22. Pancreatic β-cells. Figure 19 is a freeze–fracture replica showing numerous exocytotic sites (arrows) in the plasma membrane (PM(P)) of a cell not treated with filipin. Figures 20 to 22 show similar images in filipin-treated cells. In these sparsely labelled membranes (PM(P)), f–c complexes occur around exocytotic openings (arrows). Note the richly labelled secretory granule (GM(E)) membrane in figure 21. Figure 22 shows the merging of a filipin-labelled granule membrane (GM(E)) with the plasma membrane (PM(P)) in a filipin-containing region (see figure 15 for a similar image in untreated β-cells). (Magns: figure 19, ×52000; figure 20, ×77000; figure 21, ×47000; figure 22, ×70000.)

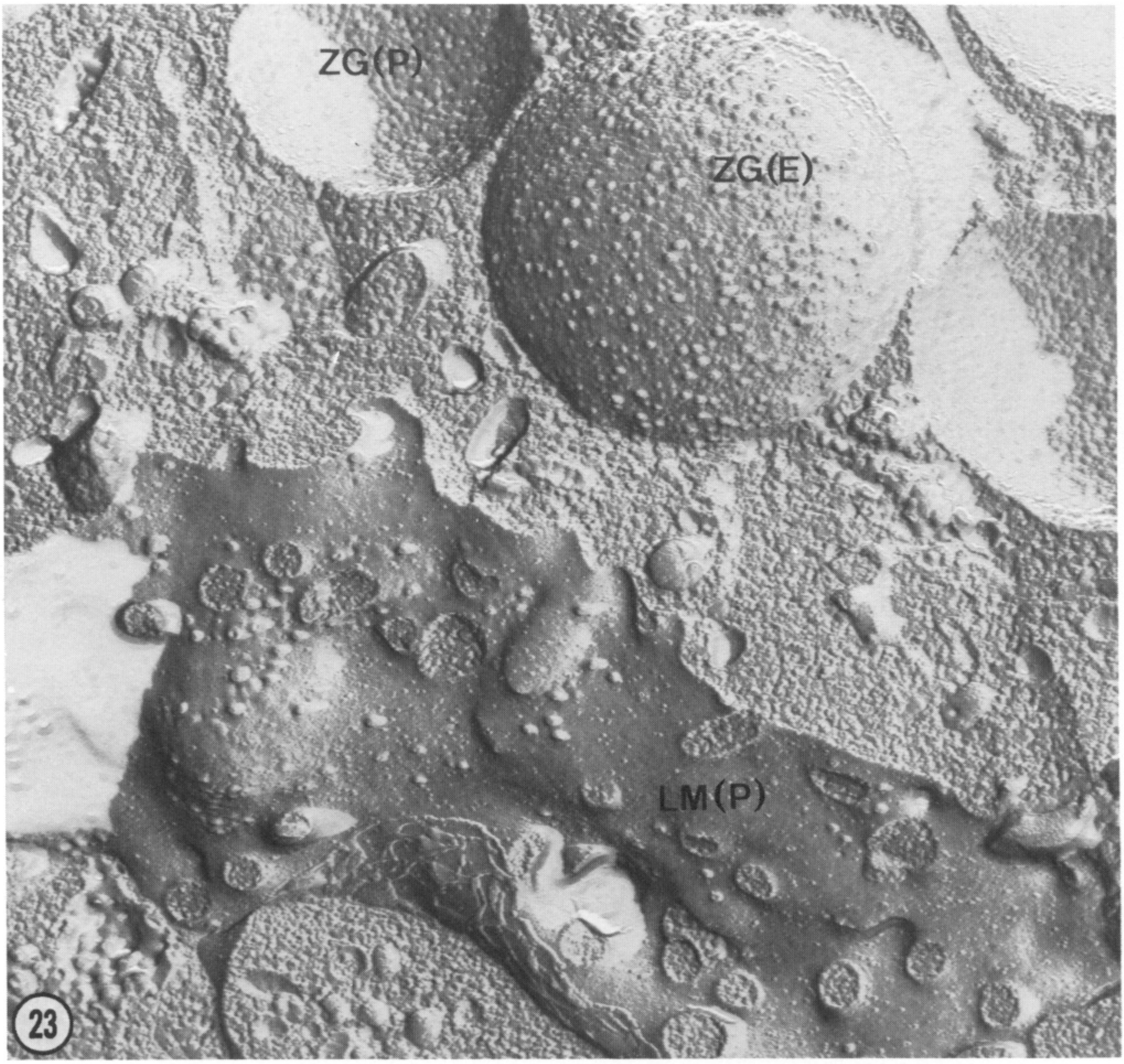

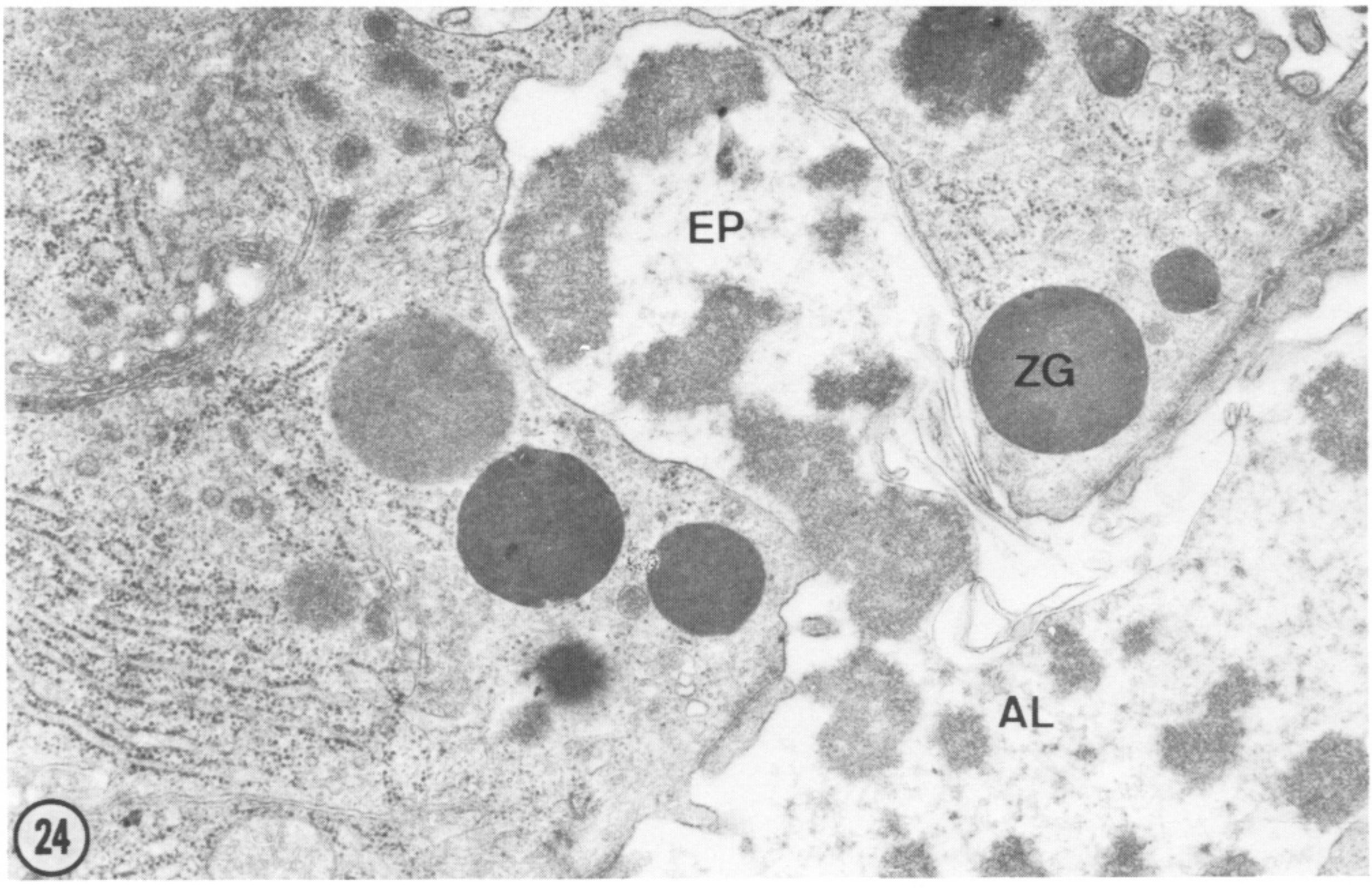

FIGURES 23 AND 24. For description see opposite.

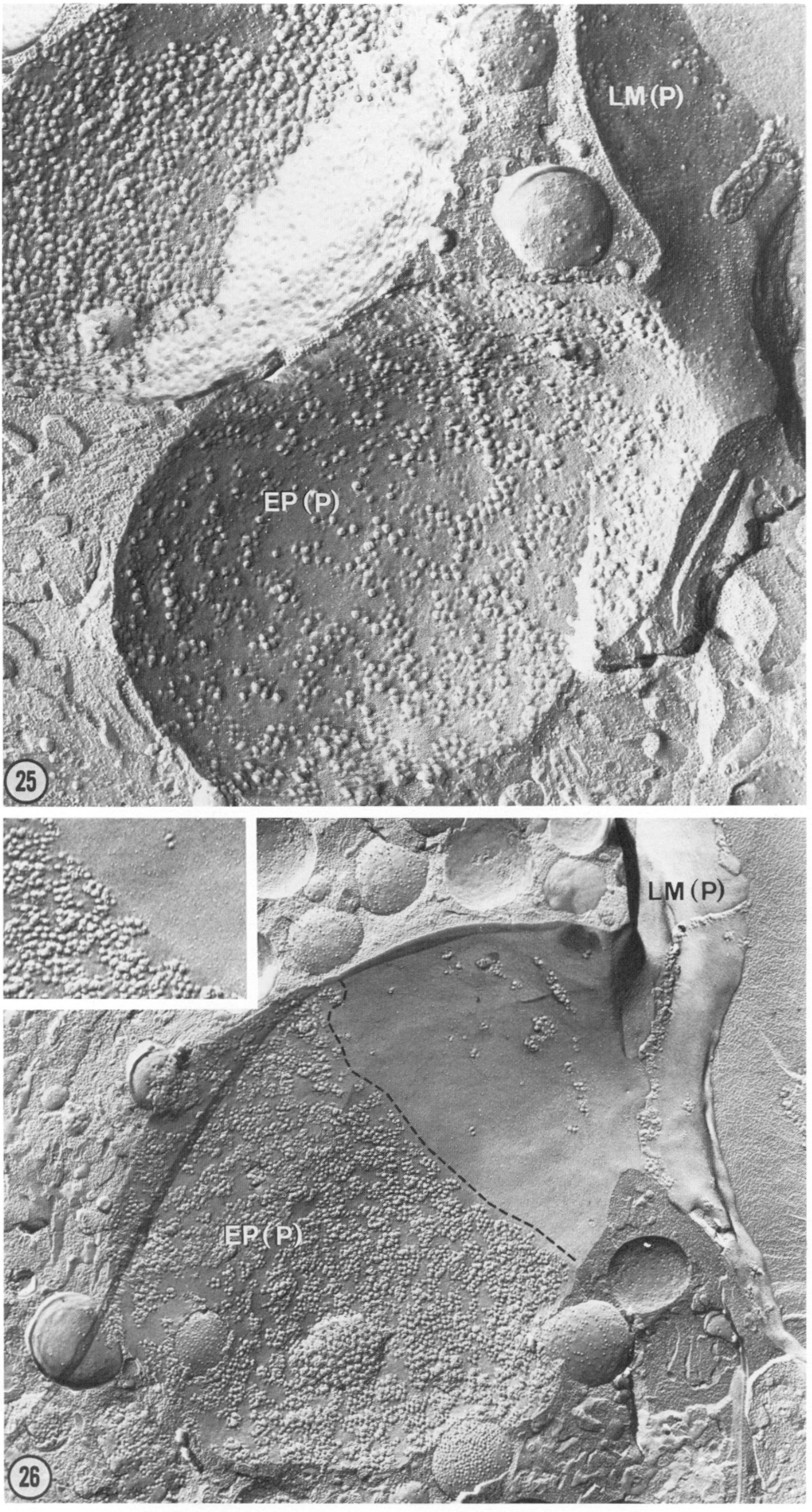

FIGURES 25 AND 26. For description see opposite.

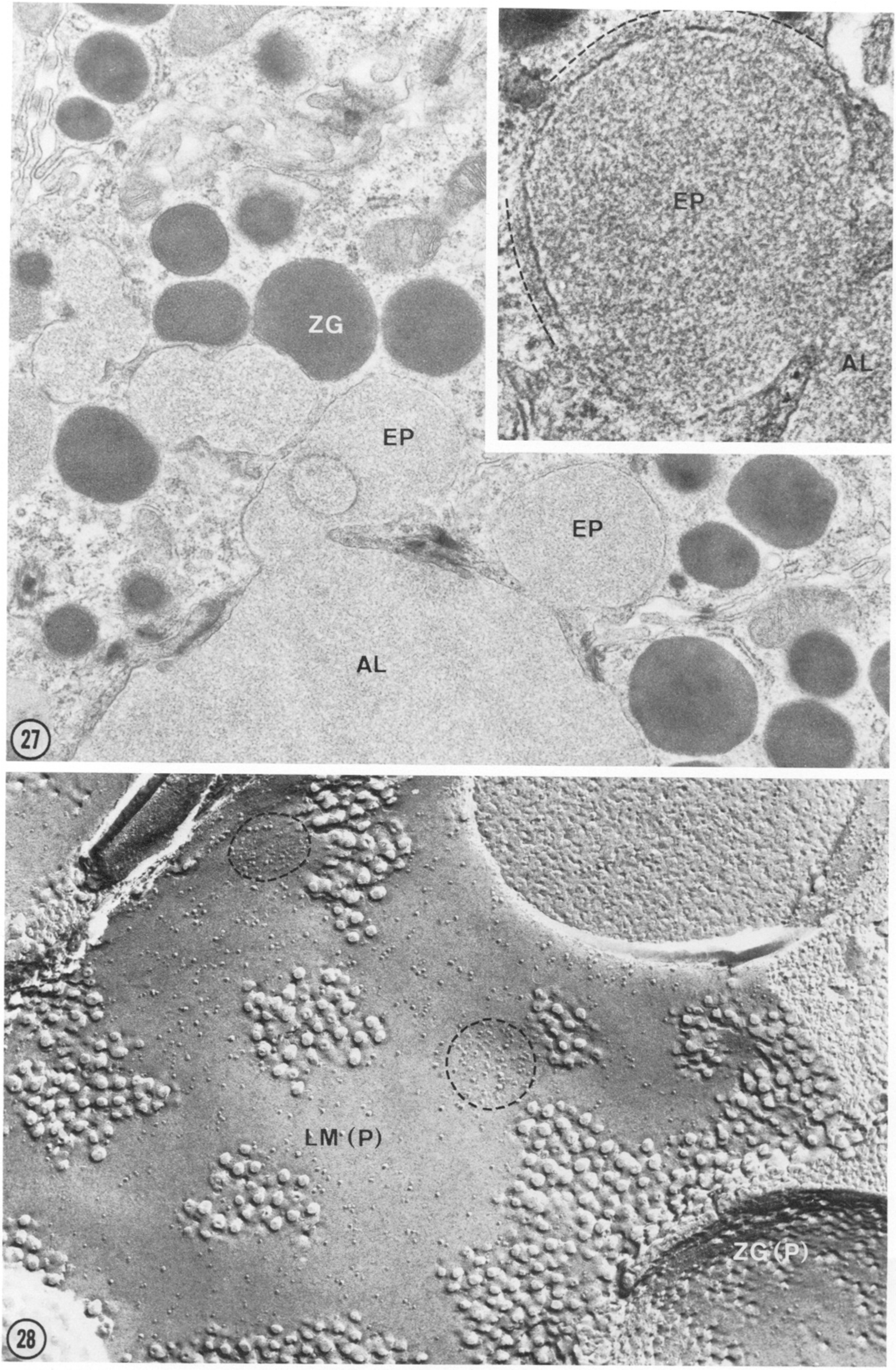

FIGURES 27 and 28. For description see opposite.

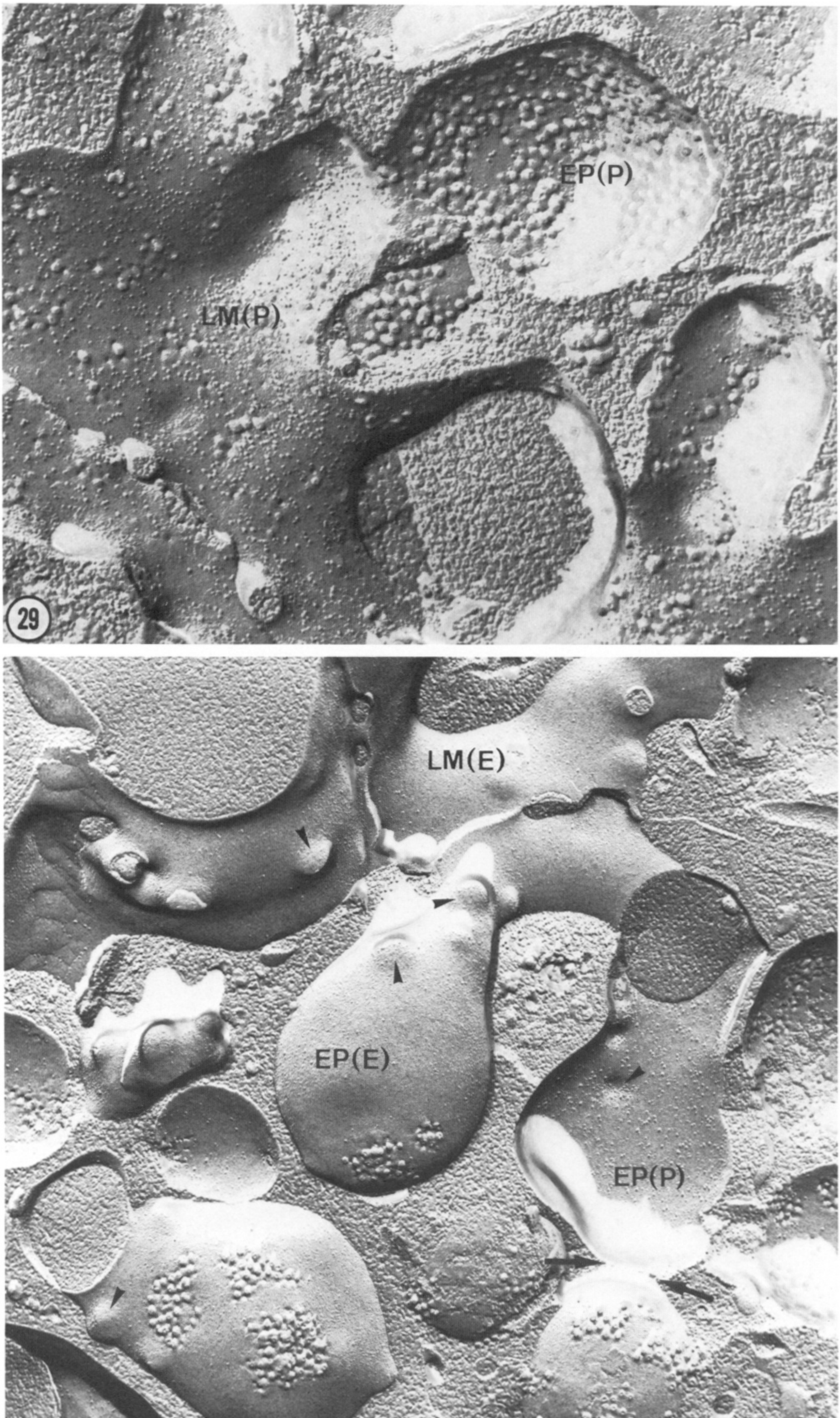

FIGURES 29 AND 30. For description see opposite.